

## Supporting information

Figure S1:

Relationship between gene family size and production of alternatively spliced variants in human. Fraction of genes containing more than one splice variant is displayed. Binning is similar to Kopelman *et al.* (6) (see also Figure 1A).

Figure S2:

Regression between gene family size and the proportion of genes undergoing alternative splicing in human. Legend similar to Figure 1. A linear regression was tested against a parabola (polynomial regression of order 2; see Methods). Both regression curves are displayed on the graph.

Figure S3:

Relationship between gene family size and the proportion of genes undergoing alternative splicing in mouse (*Mus musculus*). Legend similar to Figure 1.

Figure S4:

Relationship between gene family size and the proportion of genes undergoing alternative splicing in zebrafish (*Danio rerio*). Legend similar to Figure 1.

Figure S5:

Relationship between gene family size and the proportion of genes undergoing alternative splicing in human. Ensembl protein families were used to calculate family size. Legend similar to Figure 1.

Figure S6:

Relationship between gene family size and the proportion of genes undergoing alternative splicing in human. UCSC genome browser was used to estimate number of splice forms per gene. Legend similar to Figure 1.

Figure S7:

Relationship between gene family size and the proportion of genes undergoing alternative splicing in human. Four bins of genes were created using quartiles of EST counts (see Methods) and the trend is displayed for each sub-groups. Legend similar to Figure 1.

Figure S8:

Relationship between gene family size and the proportion of genes undergoing alternative splicing in human. Four bins of genes were created depending on their number of constitutive exons and the trend is displayed for each sub-groups. Genes with no constitutive exon are by definition all undergoing alternative splicing and are not included here. Legend similar to Figure 1.

Figure S9:

Relationship between gene family size and the proportion of genes undergoing alternative splicing in human. Four bins of genes were created using quartiles of  $d_N/d_S$  values (calculated with mouse; see Methods) and the trend is displayed for each sub-groups. Legend similar to Figure 1.

Figure S10:

Relationship between gene family size and the proportion of genes undergoing alternative splicing in human. Four bins of genes were created using quartiles of their maximum transcript length and the trend is displayed for each sub-groups. Legend similar to Figure 1.

Figure S11:

Relationship between gene family size and the proportion of genes undergoing alternative splicing in human. Recent duplicates specific to *Homo sapiens* were excluded from the dataset because they might be assembly artefacts. Legend similar to Figure 1.

Figure S12:

Relationship between mean number of alternative spliced variants and age of genes last duplication in human. Legend similar to Figure 2A. The x-axis is in shown linear-scale.

Figure S13:

Relationship between proportion of genes undergoing alternative splicing and age of genes last duplication in human. Legend similar to Figure 2.

Figure S14:

Relationship between mean number of alternative spliced variants and age of genes last duplication in human. The analysis was performed separately with the genes mapped to each top-level Gene Ontology functional categories (see Methods). Legend similar to Figure 2.

Figure S15:

Relationship between the difference of number of alternative spliced variants for gene duplicate pairs and age of genes last duplication in human. The analysis was restricted to duplicate pairs for which no later duplication occurred (see Methods). Legend similar to Figure 2.

Figure S16:

Histograms comparing the number of splice forms between genes whose last duplication is old (Bilateria; in black) and genes whose last duplication is recent (*Homo sapiens*; in gray).

Figure S17:

Relationship between proportion of singleton genes undergoing alternative splicing and their age in human. Legend similar to Figure 2.

Figure S18:

Relationship between mean number of alternative spliced variants and age of singletons in human. Legend similar to Figure 2B. The x-axis is in shown linear-scale.

Figure S19:

Relationship between mean number of alternative spliced variants and age of singletons in human. Four bins of genes were created using quartiles of  $d_N/d_S$  values (calculated with mouse; see Methods) and the trend is displayed for each sub-groups. Legend similar to Figure 2.

Figure S20:

(A) Comparison of proportion of genes undergoing alternative splicing for groups of genes with different evolutionary histories in human. “Duplicates” are genes that kept in duplicate after the whole-genome duplications ancestral to vertebrates (2R; later duplications allowed).

“Singletons” are genes whose duplicate was not retained after 2R whole-genome duplications (later duplications not allowed). “Singletons (+ later duplications)” represent genes whose duplicate was not retained after 2R whole-genome duplications, but later duplications were experienced.

(B) Comparison of mean number of alternative spliced variants for groups of genes with different evolutionary histories in human.

Legend similar to Figure 1.

Figure S21:

Relationship between mean number of alternative spliced variants and age of genes last duplication in human. Only Ensembl transcripts encoding for a protein were kept in the dataset. Legend similar to Figure 2.

Figure S22:

(A) Relationship between proportion of genes undergoing alternative splicing and age of genes last duplication in human. Only alternative splice forms annotated by Swiss-Prot as “experimentally validated” were kept in the dataset.

(B) Relationship between mean number of alternative spliced variants and age of genes last duplication in human. Only alternative splice forms annotated by Swiss-Prot as “experimentally validated” were kept in the dataset. Legend similar to Figure 2.

Figure S23:

(A) Relationship between proportion of genes undergoing alternative splicing and age of genes last duplication in human. Only alternative splice forms conserved with mouse (extracted from the H-DBAS database) were kept in the dataset.

(B) Relationship between mean number of alternative spliced variants and age of genes last duplication in human. Only alternative splice forms conserved with mouse (extracted from the H-DBAS database) were kept in the dataset. Legend similar to Figure 2.

Figure S24:

Comparison of linear regression models explaining the mean number of alternative spliced variants by the age of singletons in human. Data were split in sub-groups and the curves are displayed for each sub-group (see legend on the graph).

- (A) Linear models were adjusted on four bins of genes depending on number of constitutive exons (see Figure S8).
- (B) Linear models were adjusted on four bins of genes depending on maximum transcript length (see Figure S10).
- (C) Linear models were adjusted on four bins of genes depending on  $d_N/d_S$  values (see Figures S9 and S19).
- (D) Linear models were adjusted on four bins of genes depending on EST counts (see Figure S7).
- (E) Linear models were adjusted on four datasets where only splice forms corresponding to a given type of splicing events (e.g., cassette exons, CE) were kept.

Figure S25:

- (A) Relationship between mean number of alternative spliced variants and the age of human genes whose last duplication occurred in the branch leading to *Homo sapiens*.
- (B) Relationship between mean number of alternative spliced variants and the age of human genes whose last duplication occurred in the branch leading to Eutheria.

Legend similar to Figure 2.

Figure S26:

Relationship between mean rate of sequence evolution (mean  $\log d_N/d_S$ ) of singleton genes and their age in human. Legend similar to Figure 2.

Figure S27:

Relationship between gene age and production of alternatively spliced variants in *Drosophila melanogaster*.

- (A) Legend as in Figure 2A.
- (B) Legend as in Figure S17.

Dataset S1:

Excel file gathering the dataset used for this study.

# Figure S1

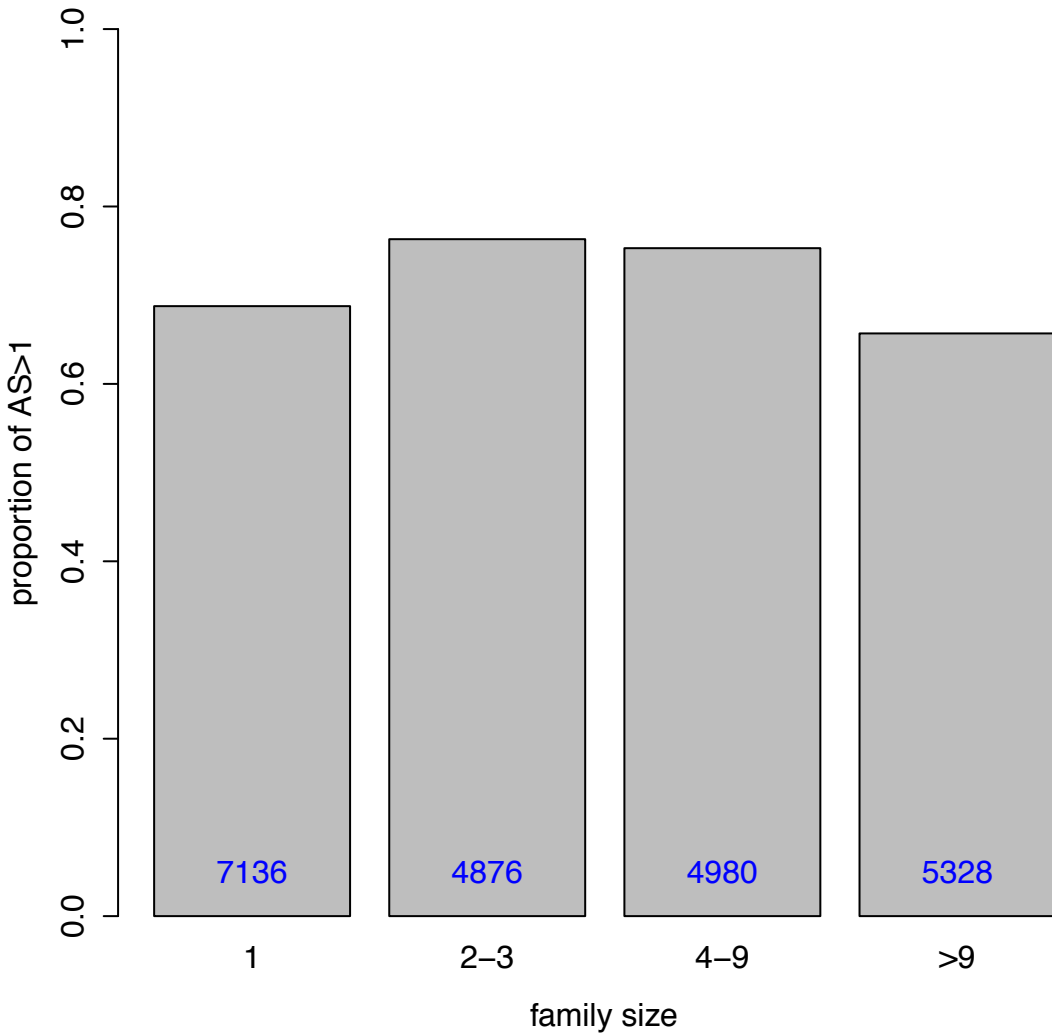
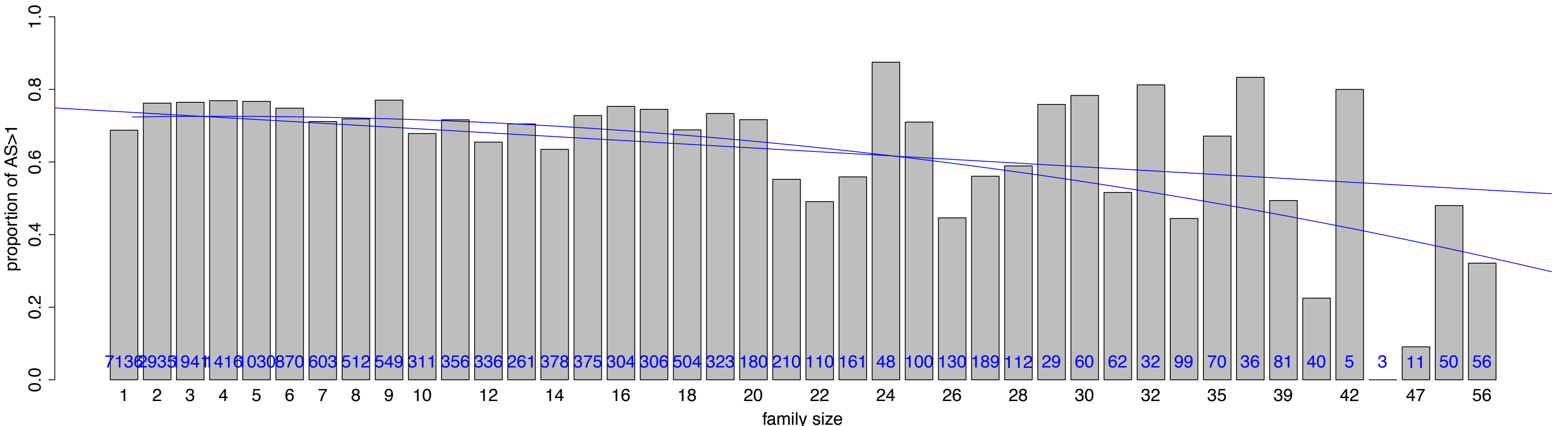
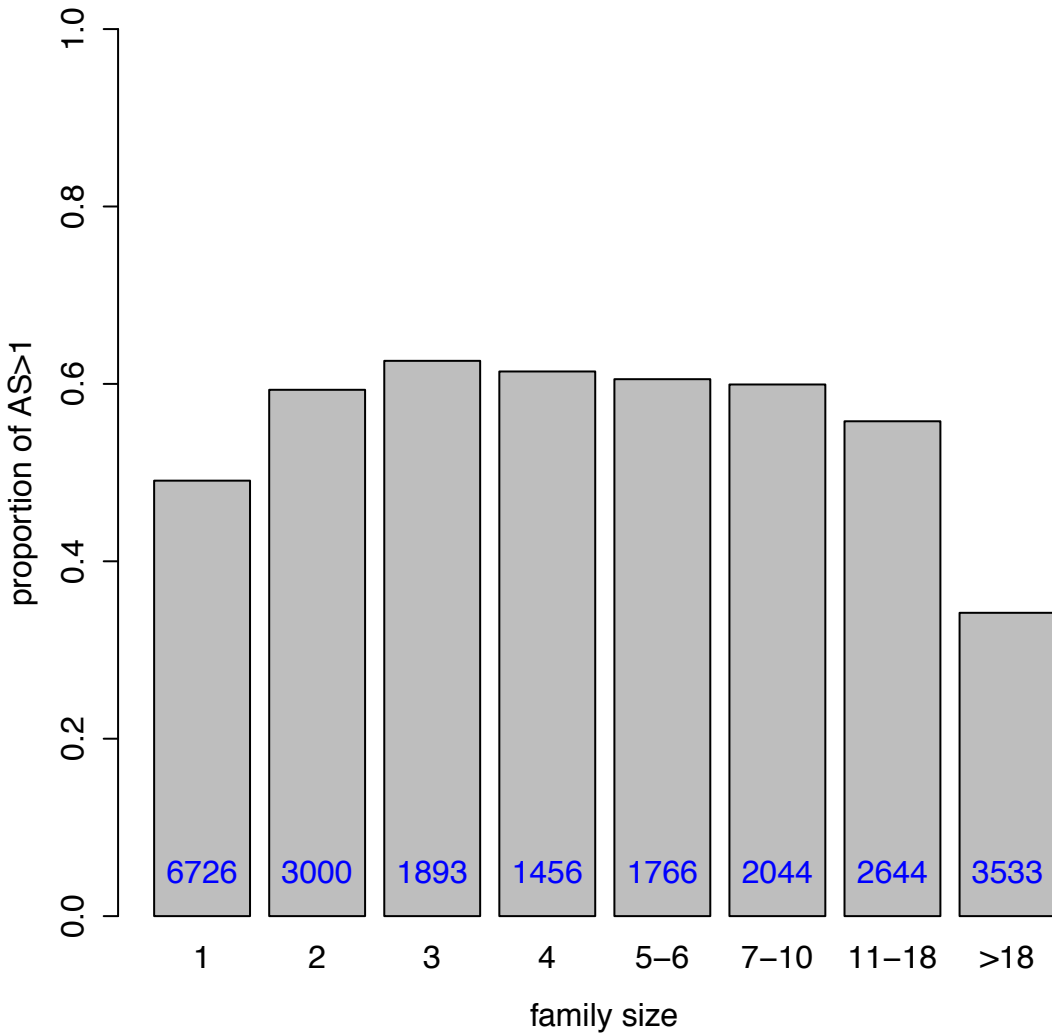


Figure S2



# Figure S3



# Figure S4

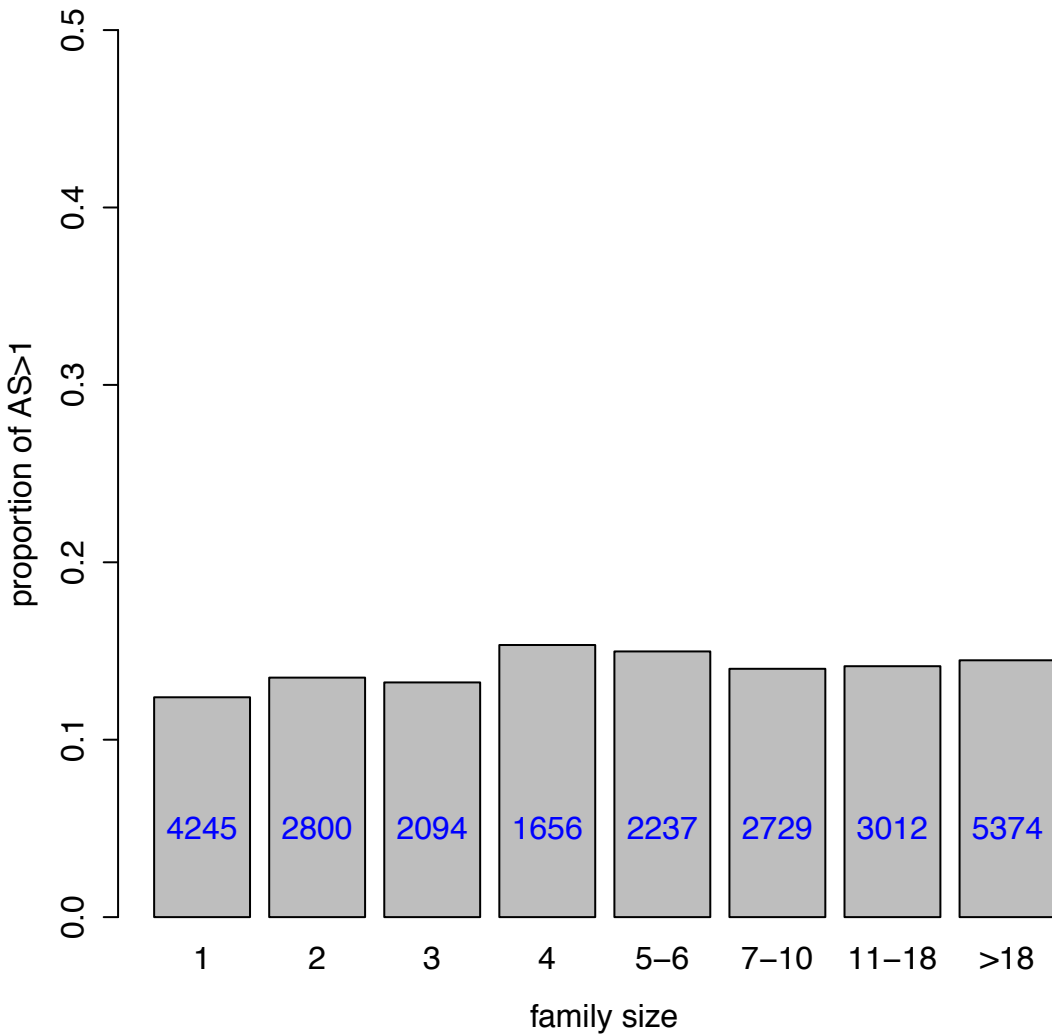


# Figure S5

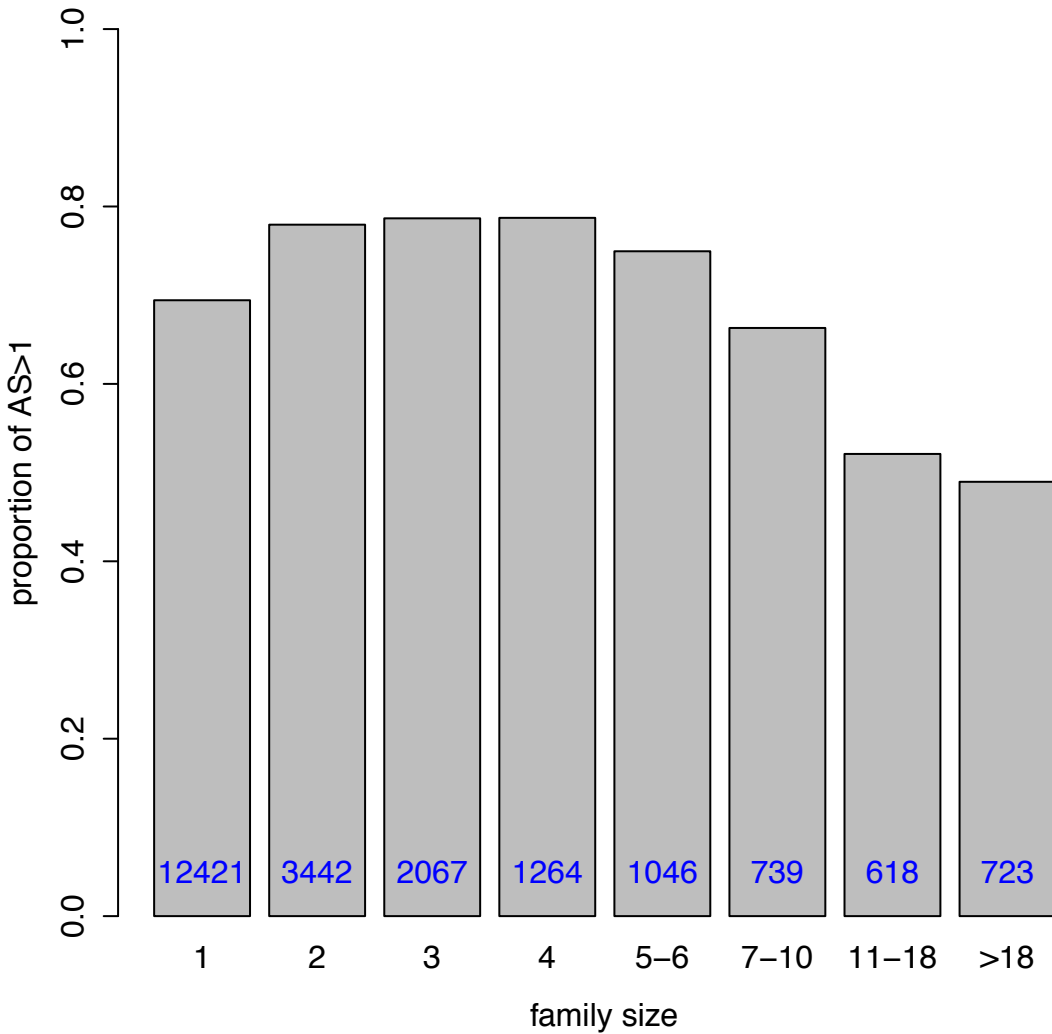


# Figure S6

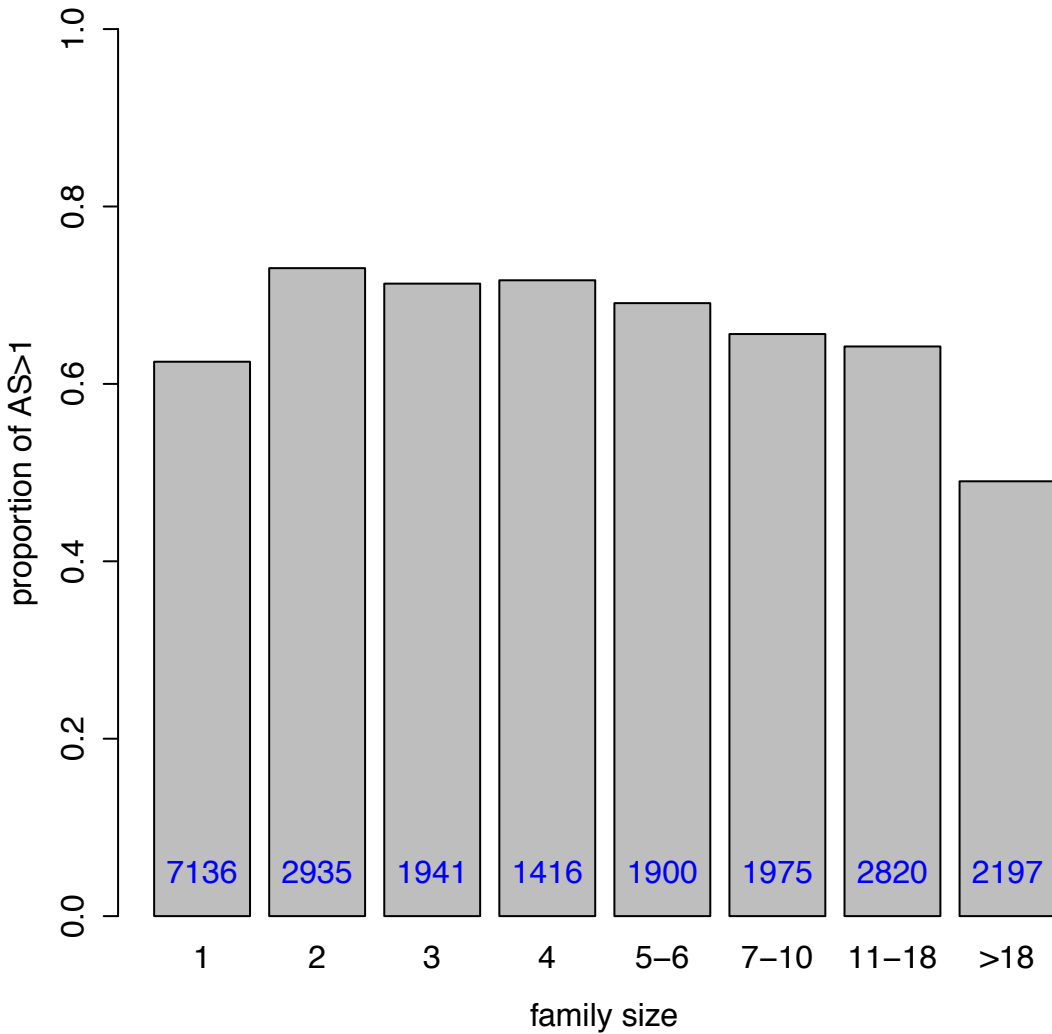
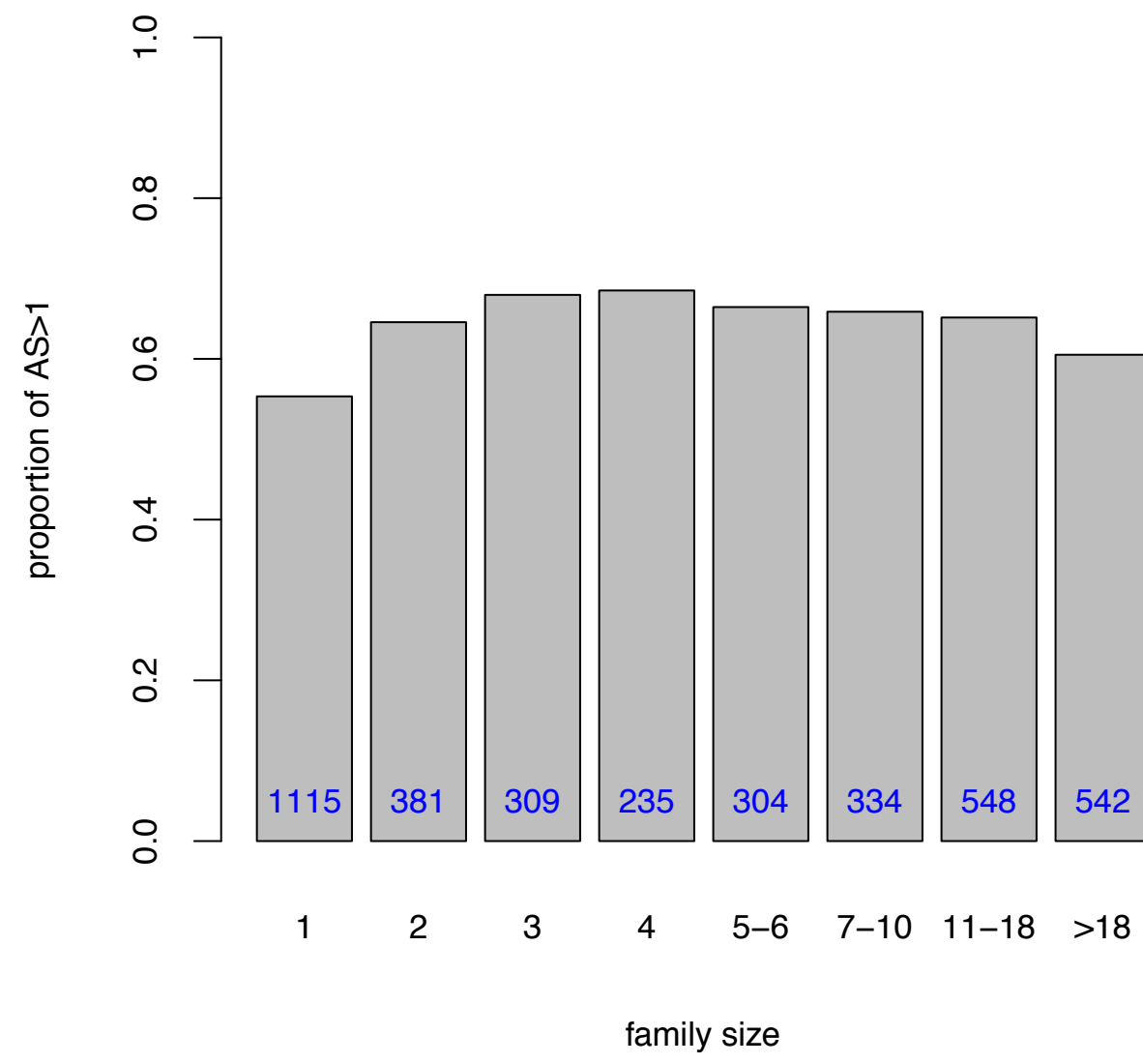
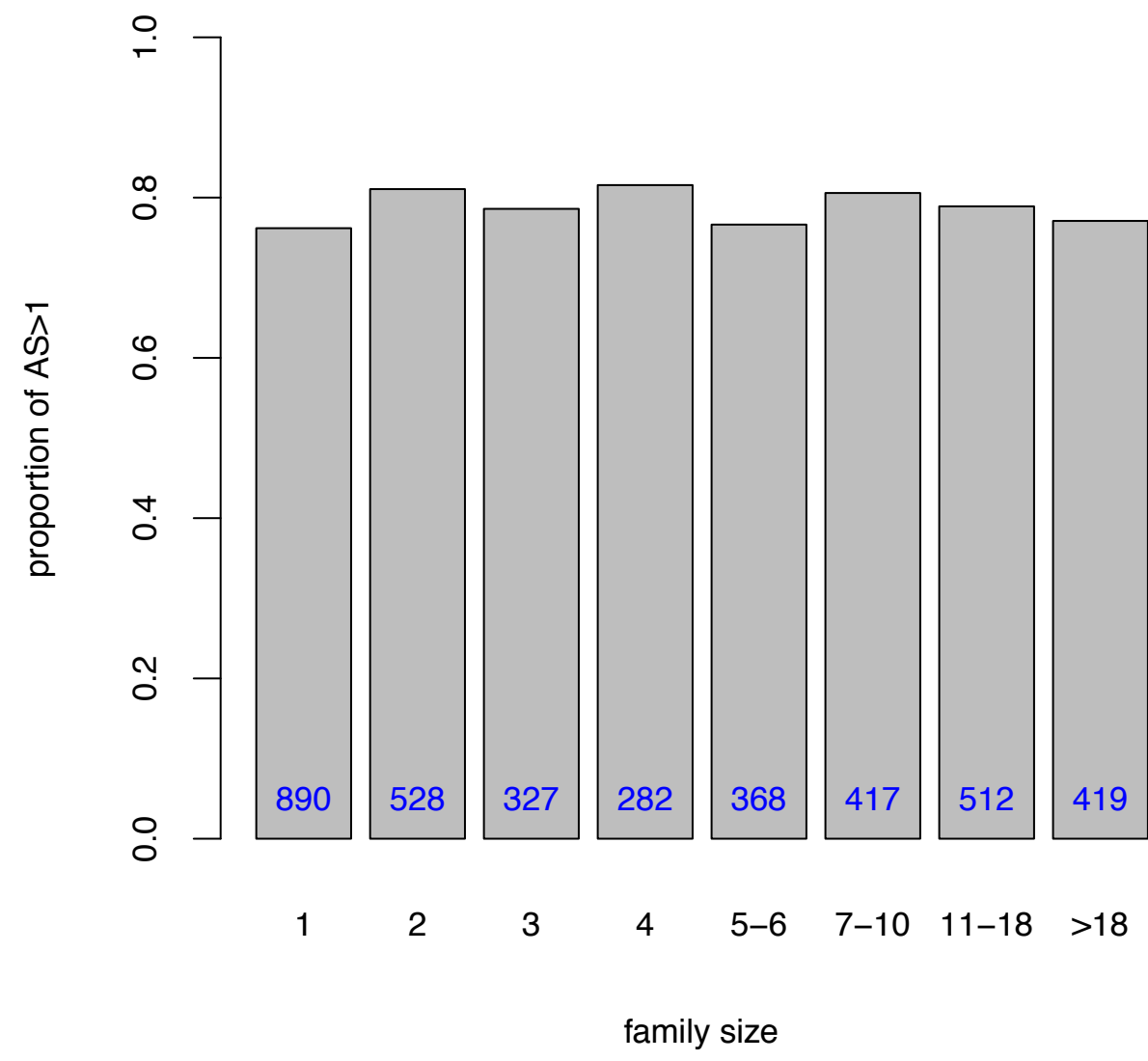


Figure S7

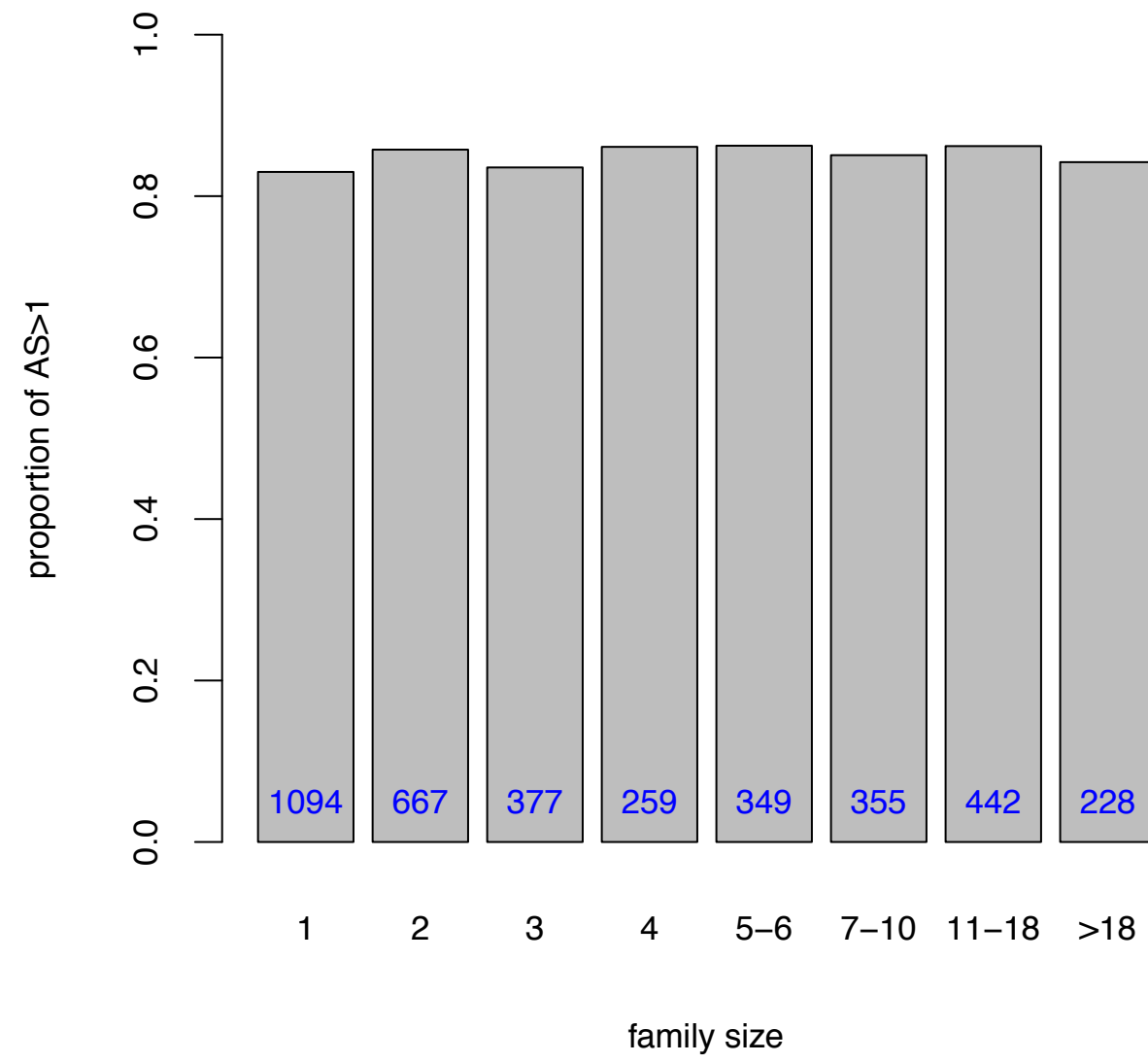
**1–14**



**15–47**



**48–103**



**>103**

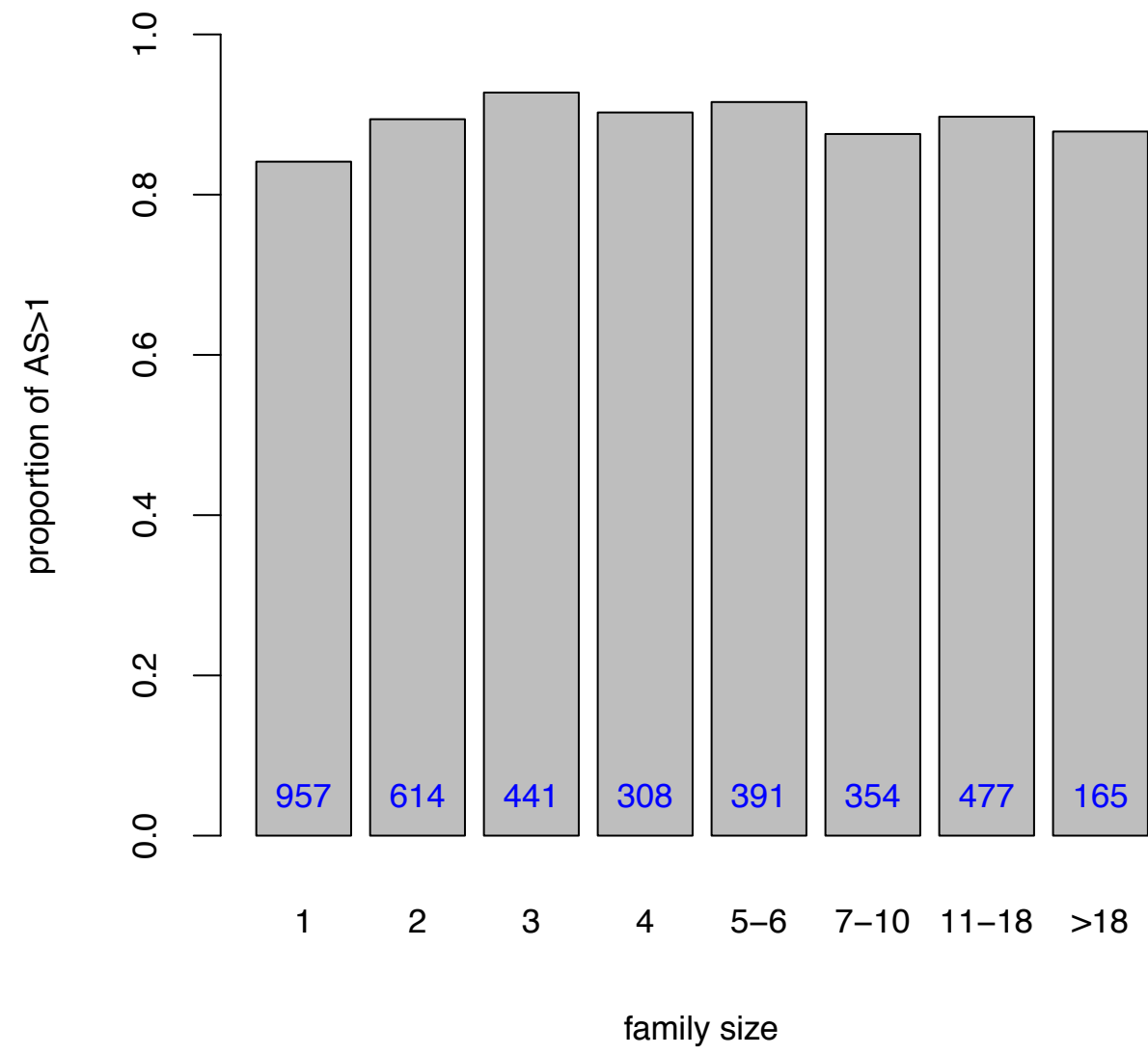
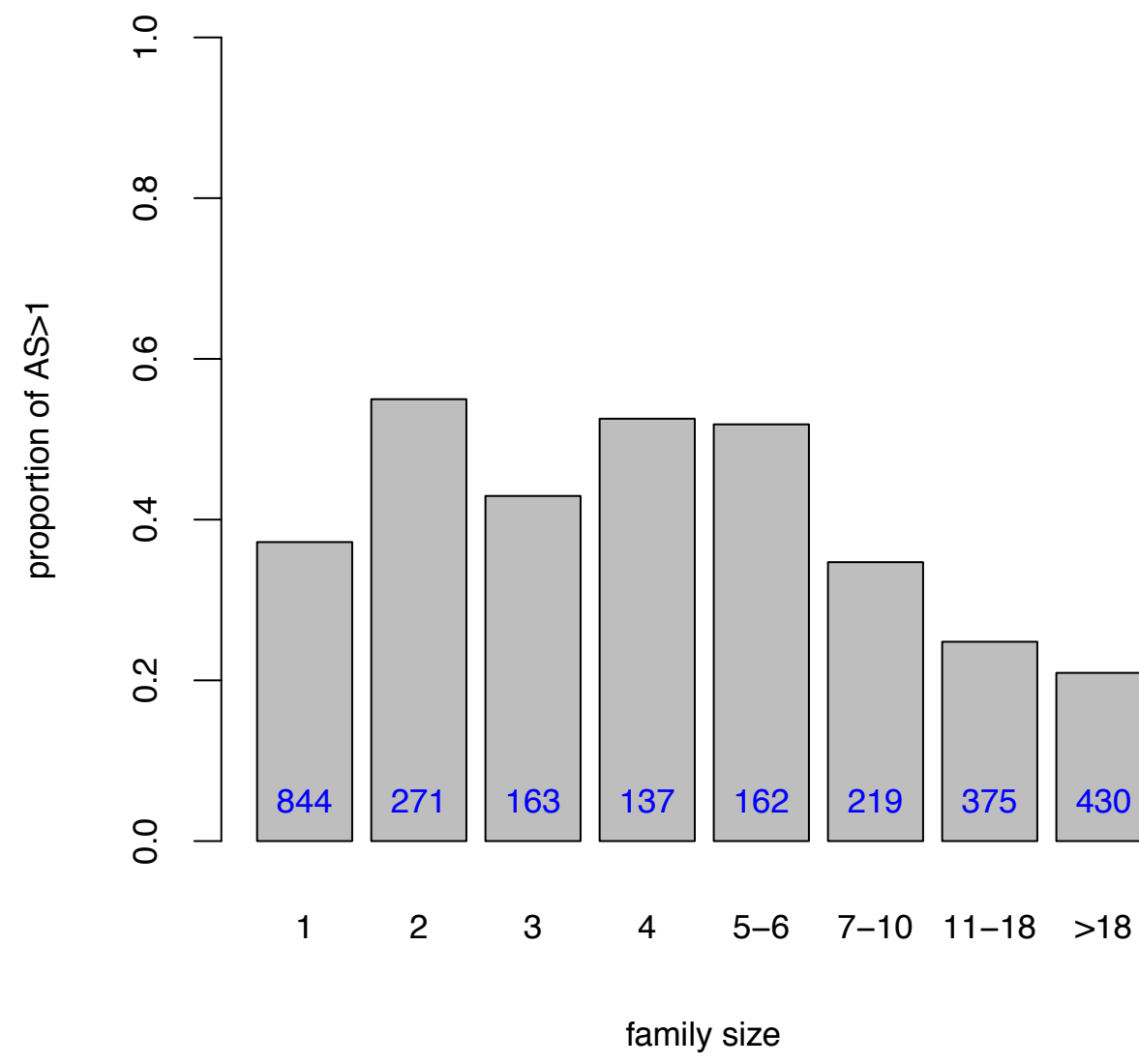
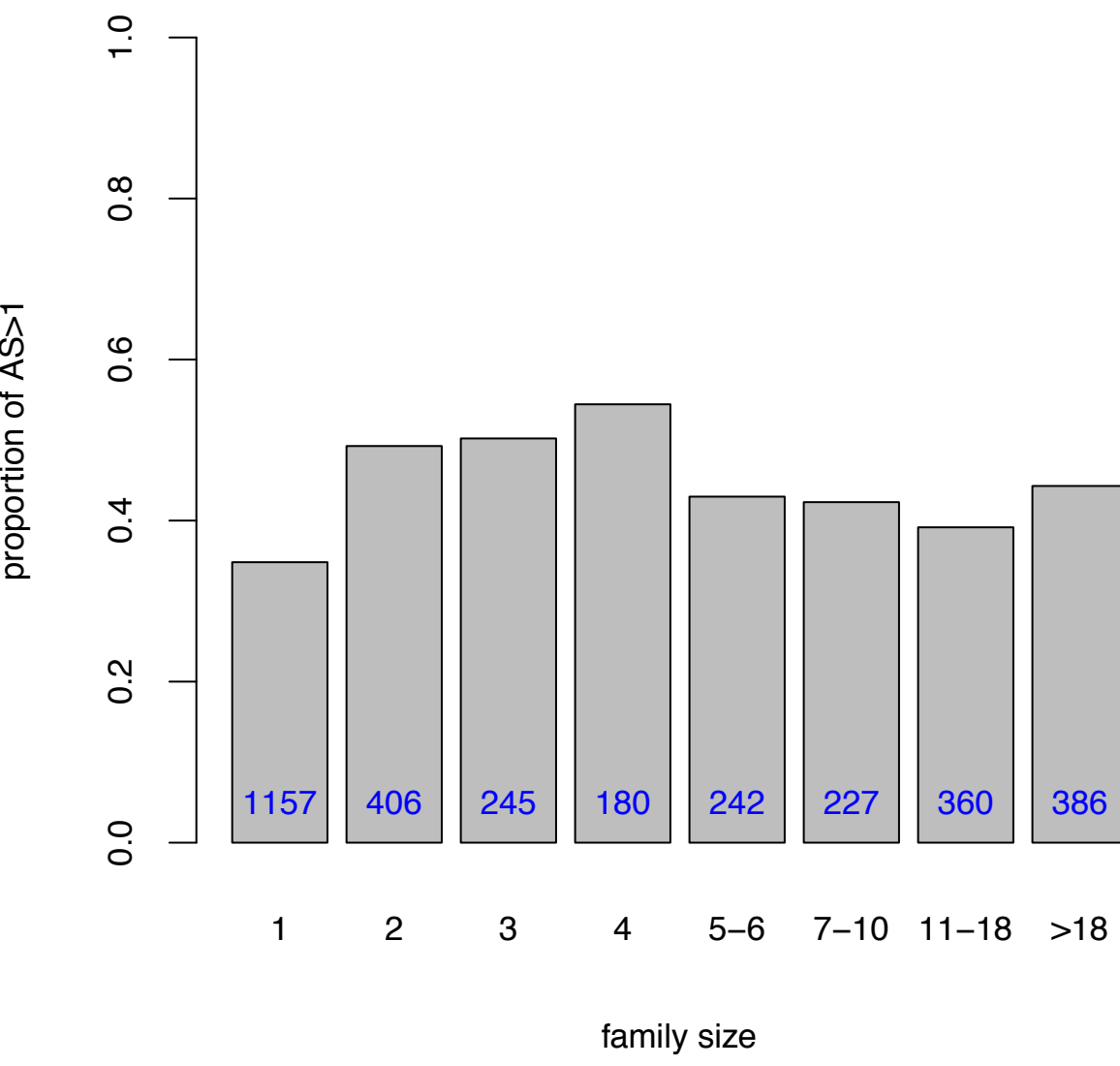


Figure S8

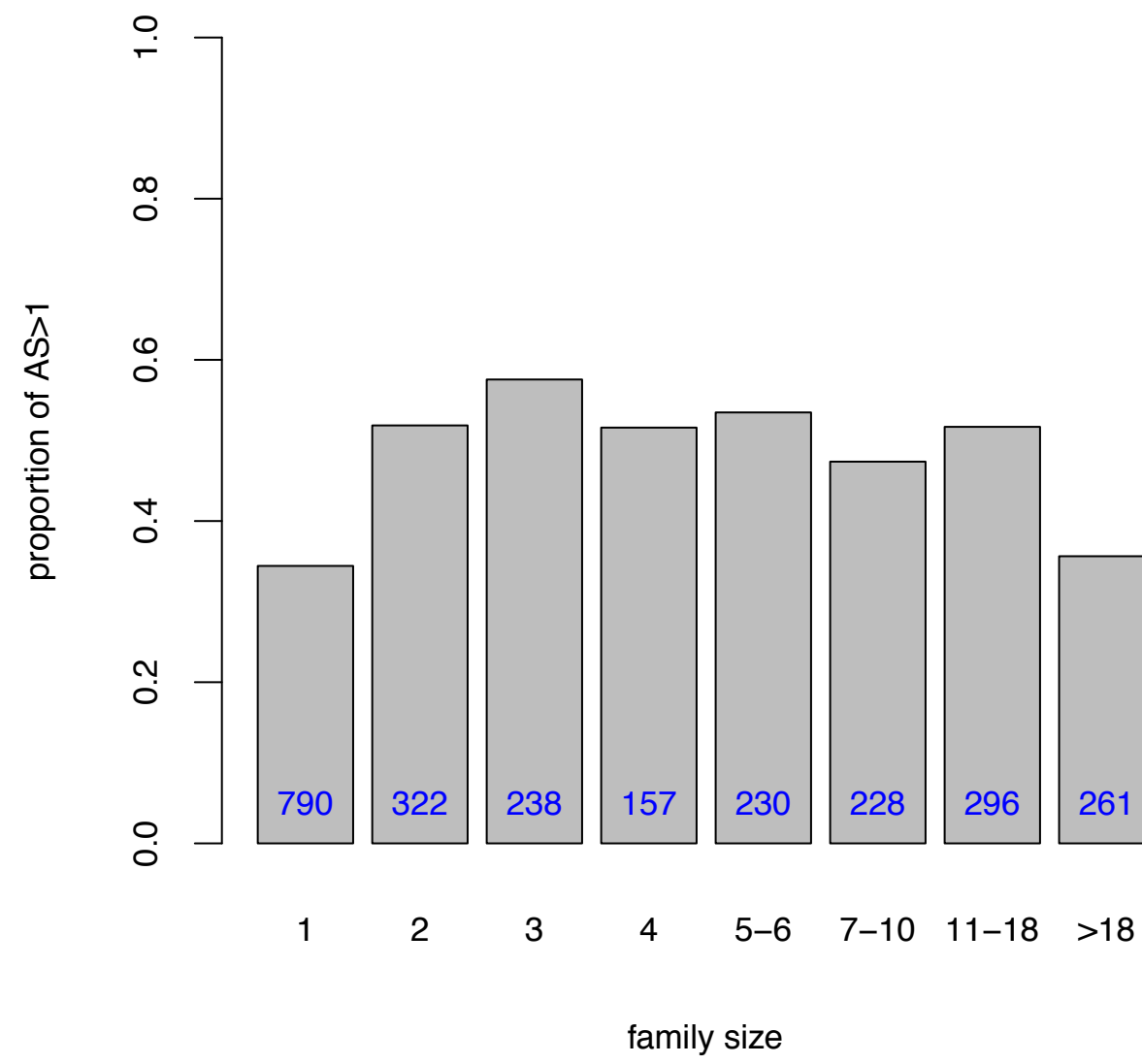
1



2-3



4-6



≥6

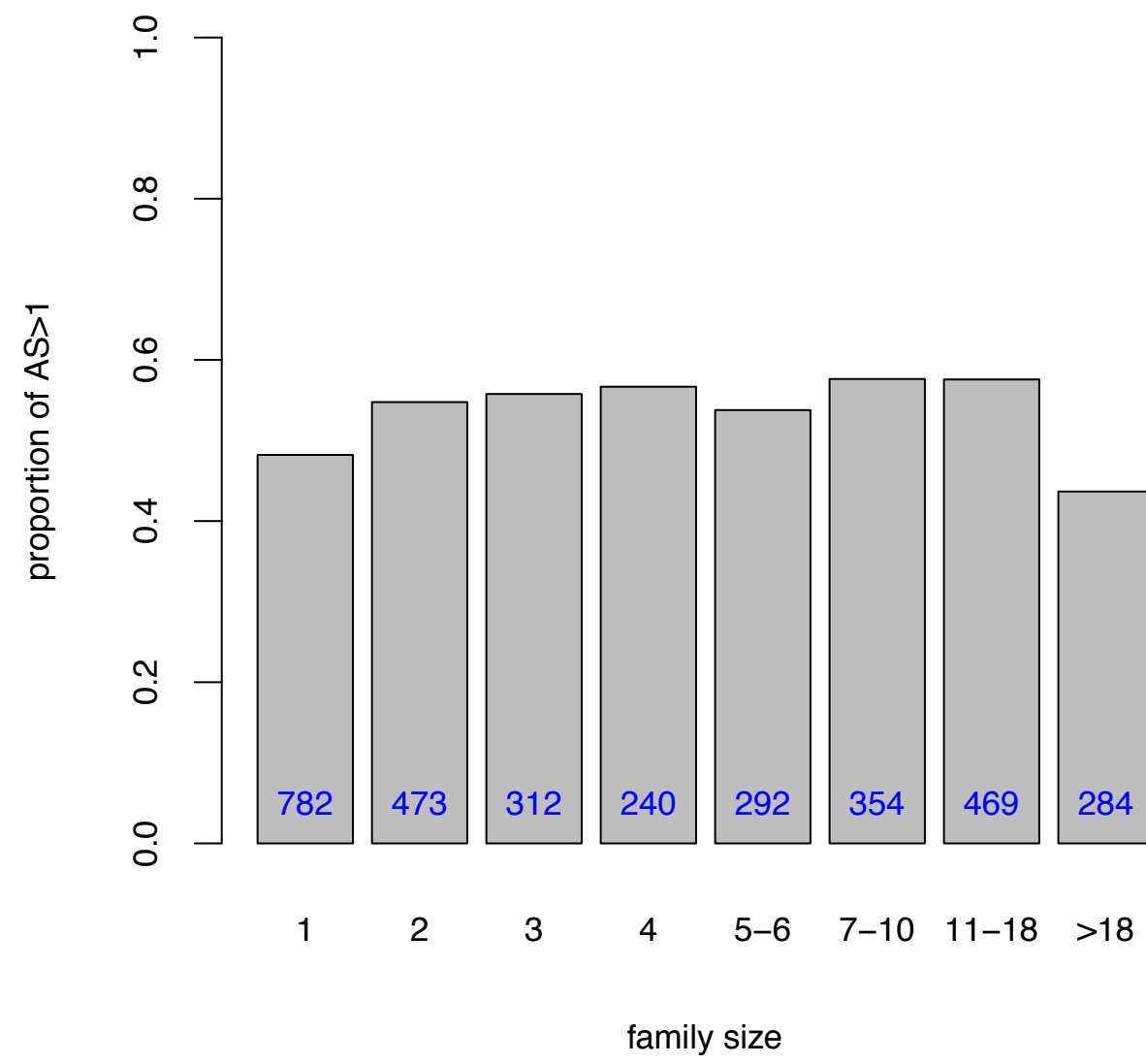
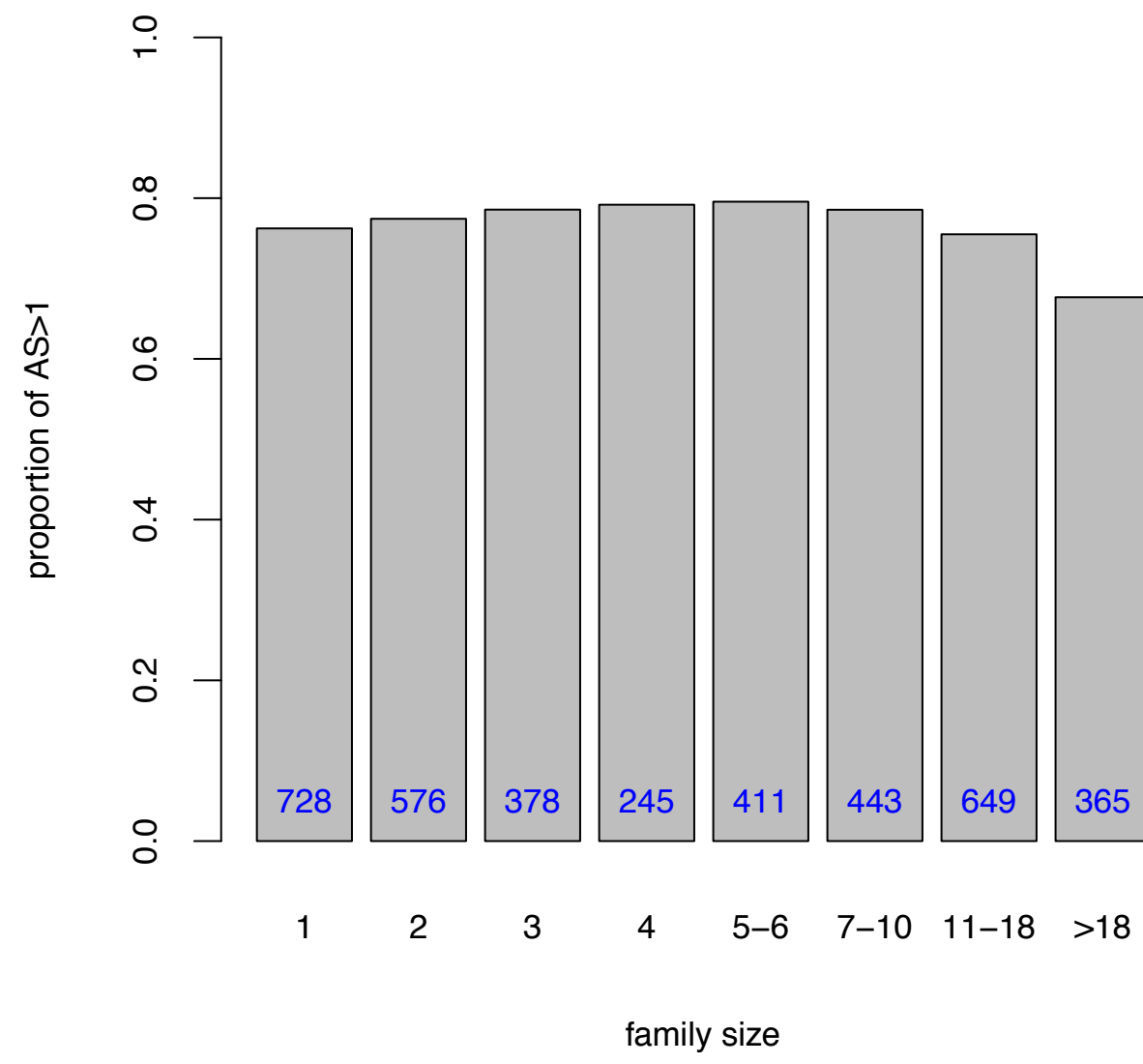
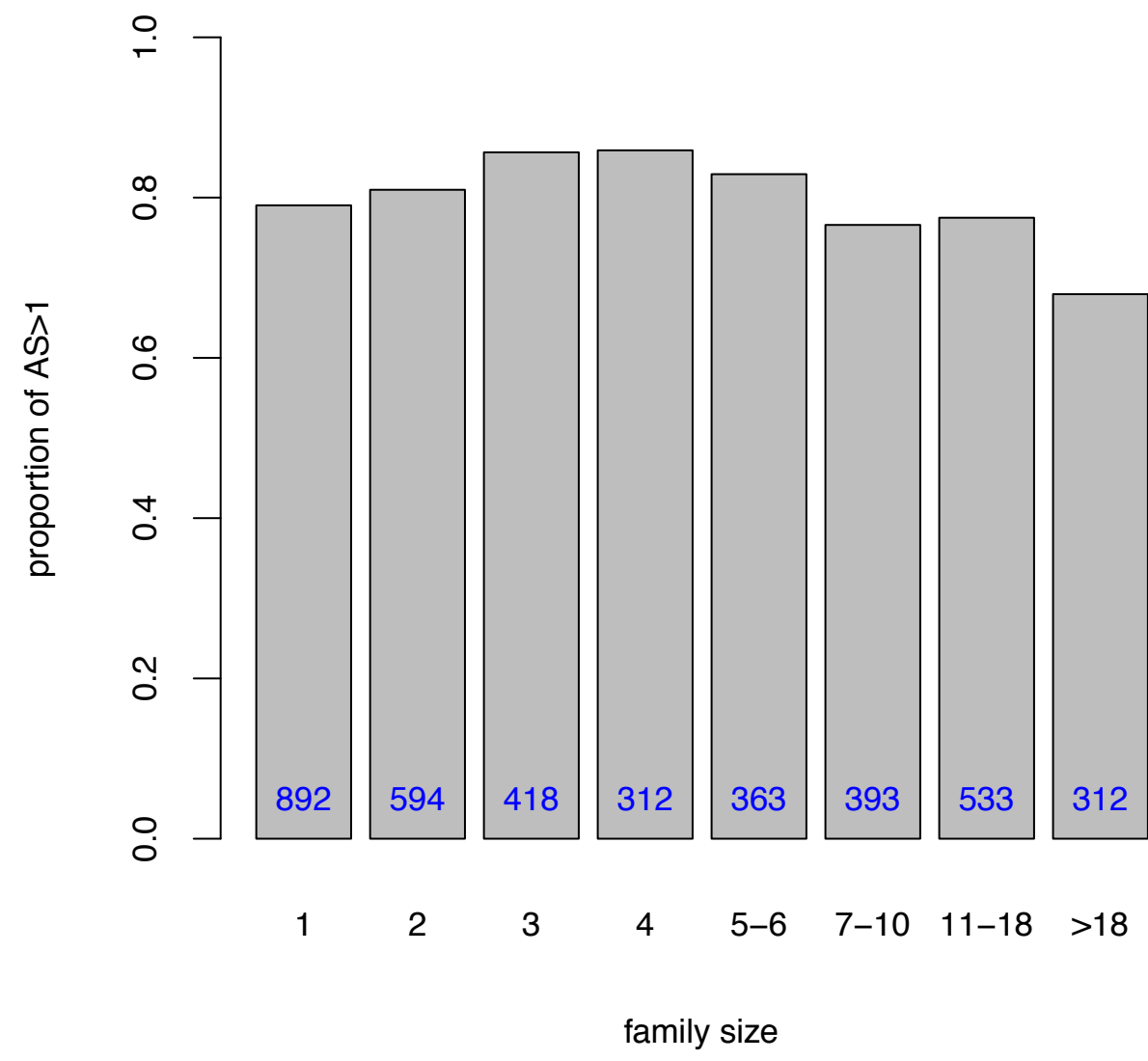


Figure S9

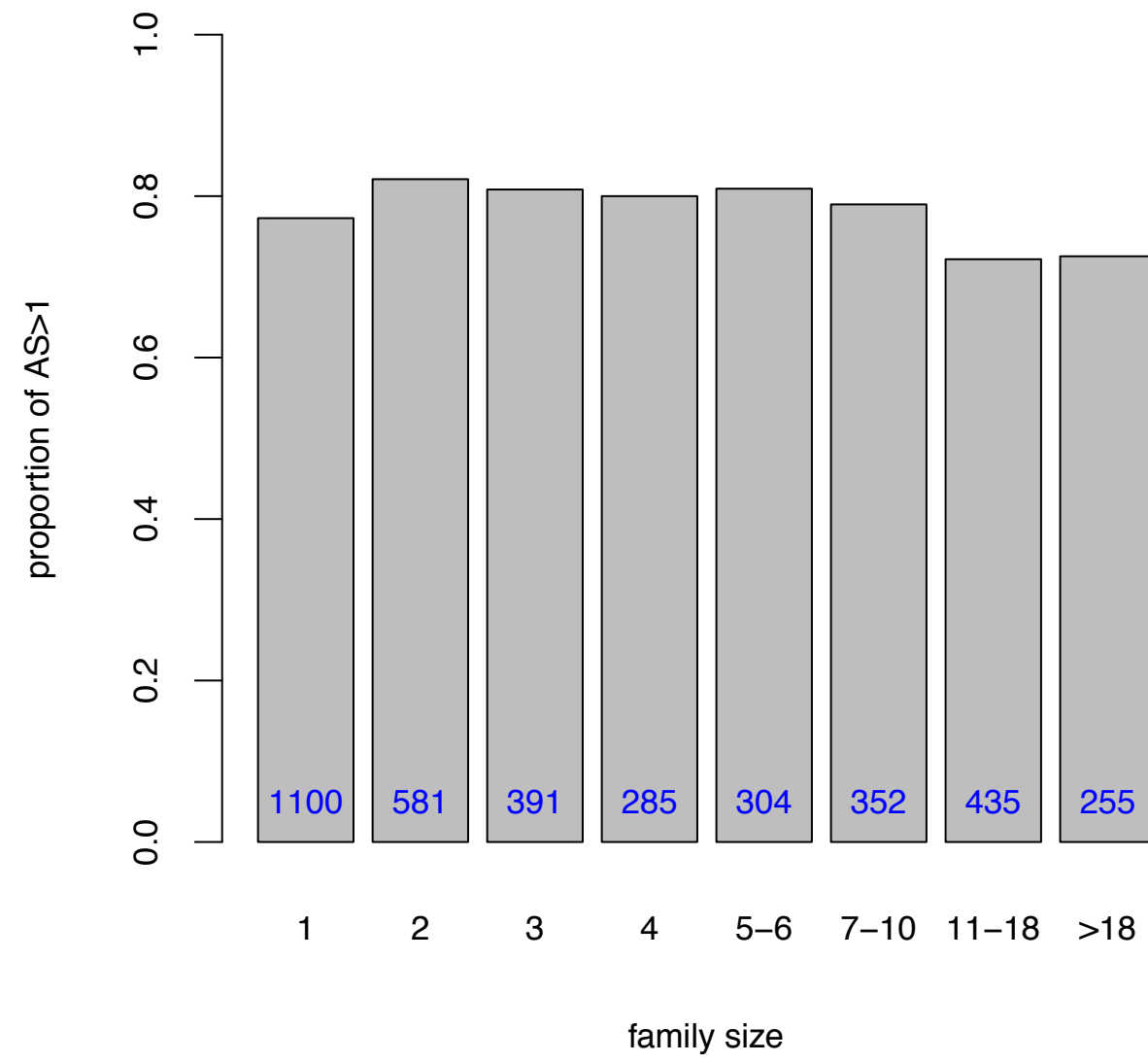
0-0.05



0.05-0.11



0.11-0.2



>0.2

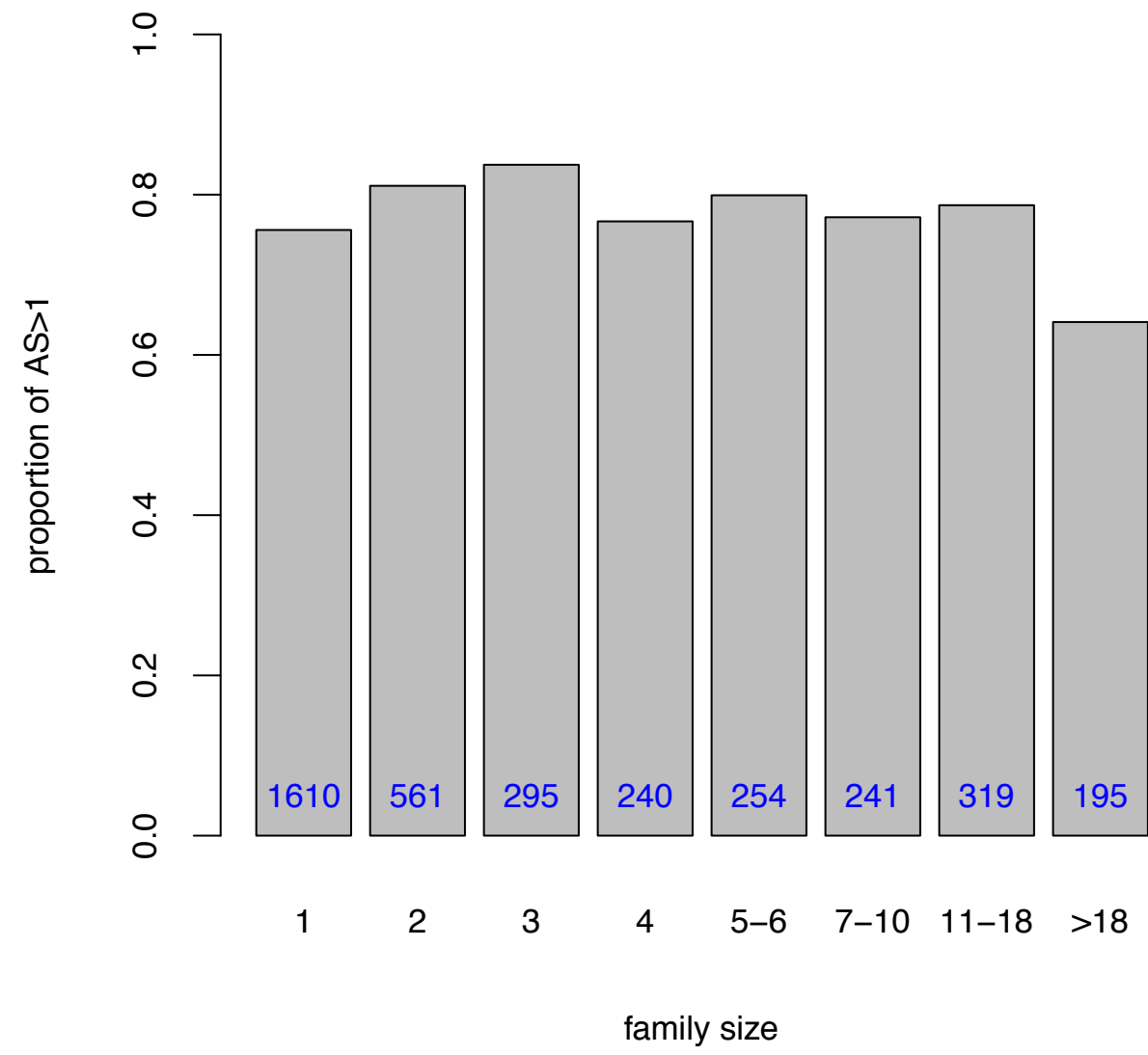
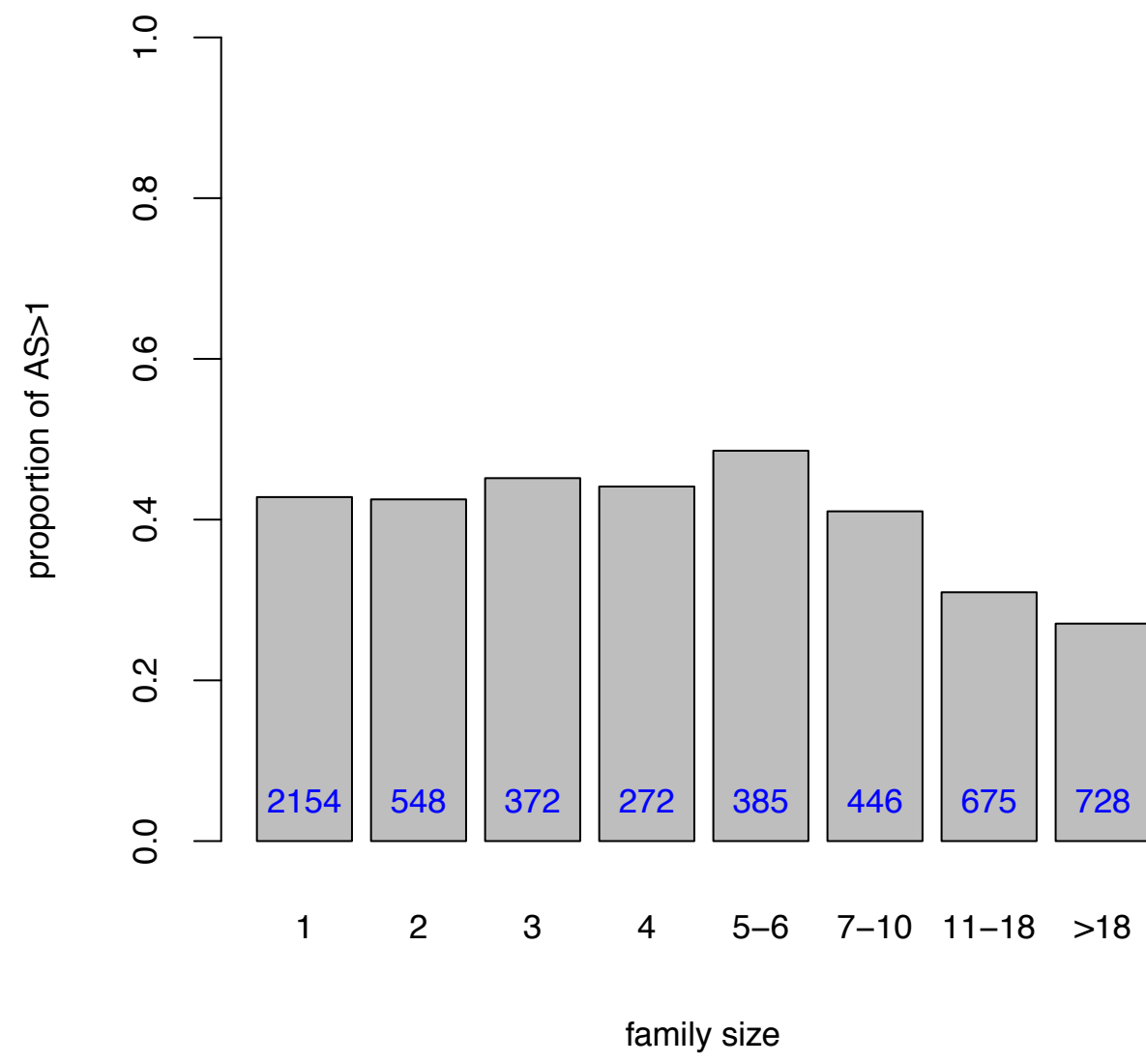
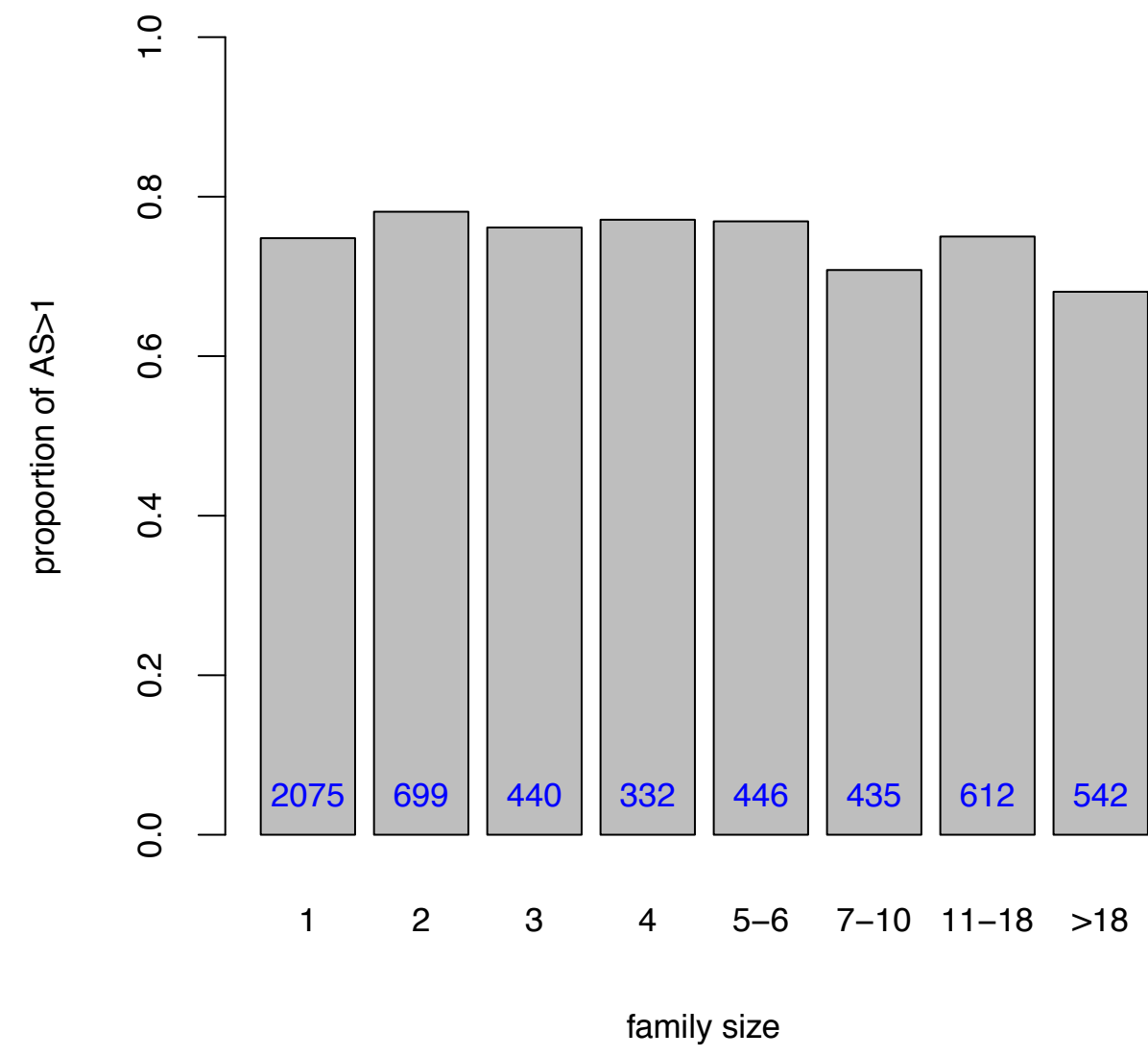


Figure S10

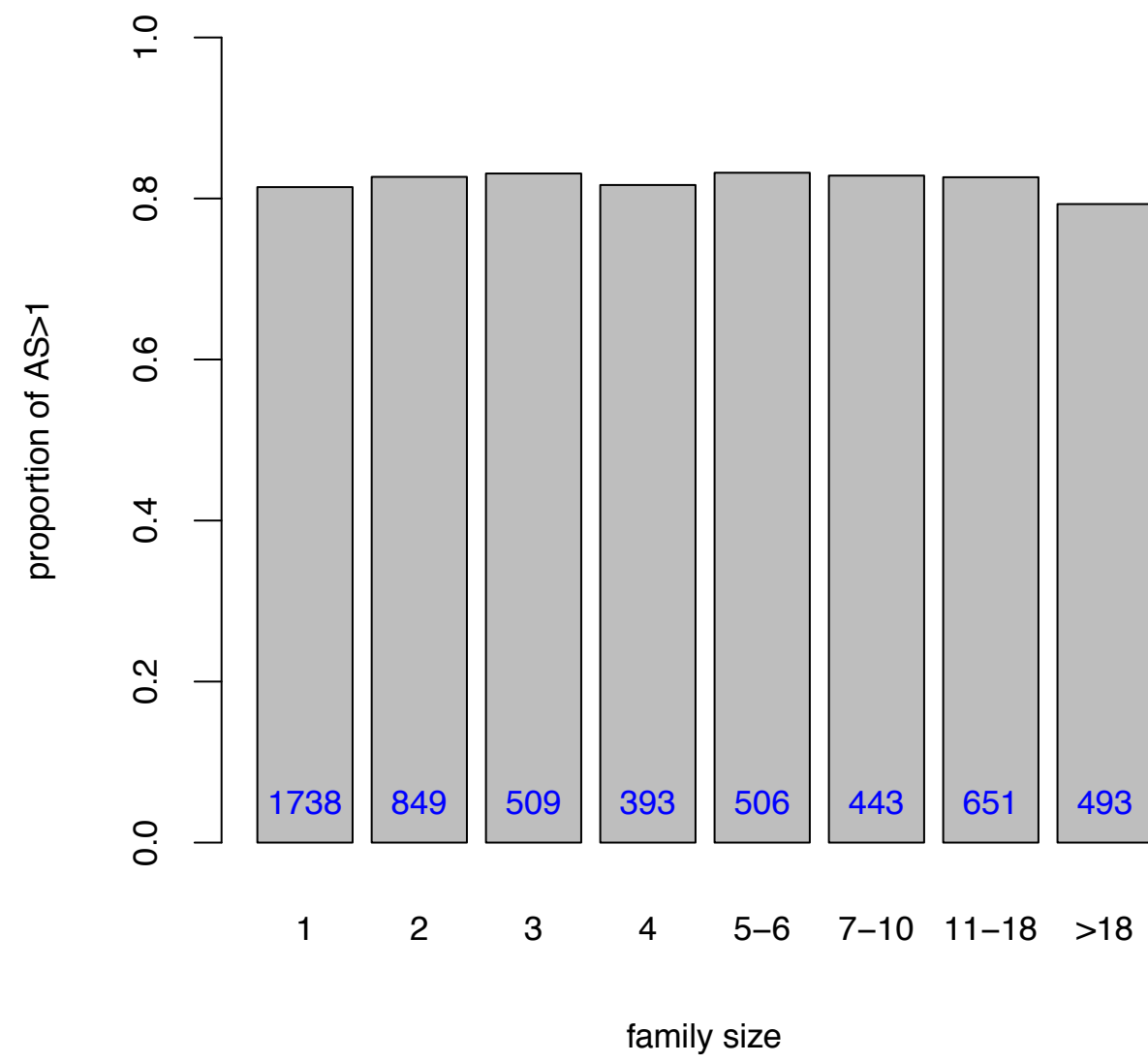
0–6324



6325–20260



20261–57070



>57070

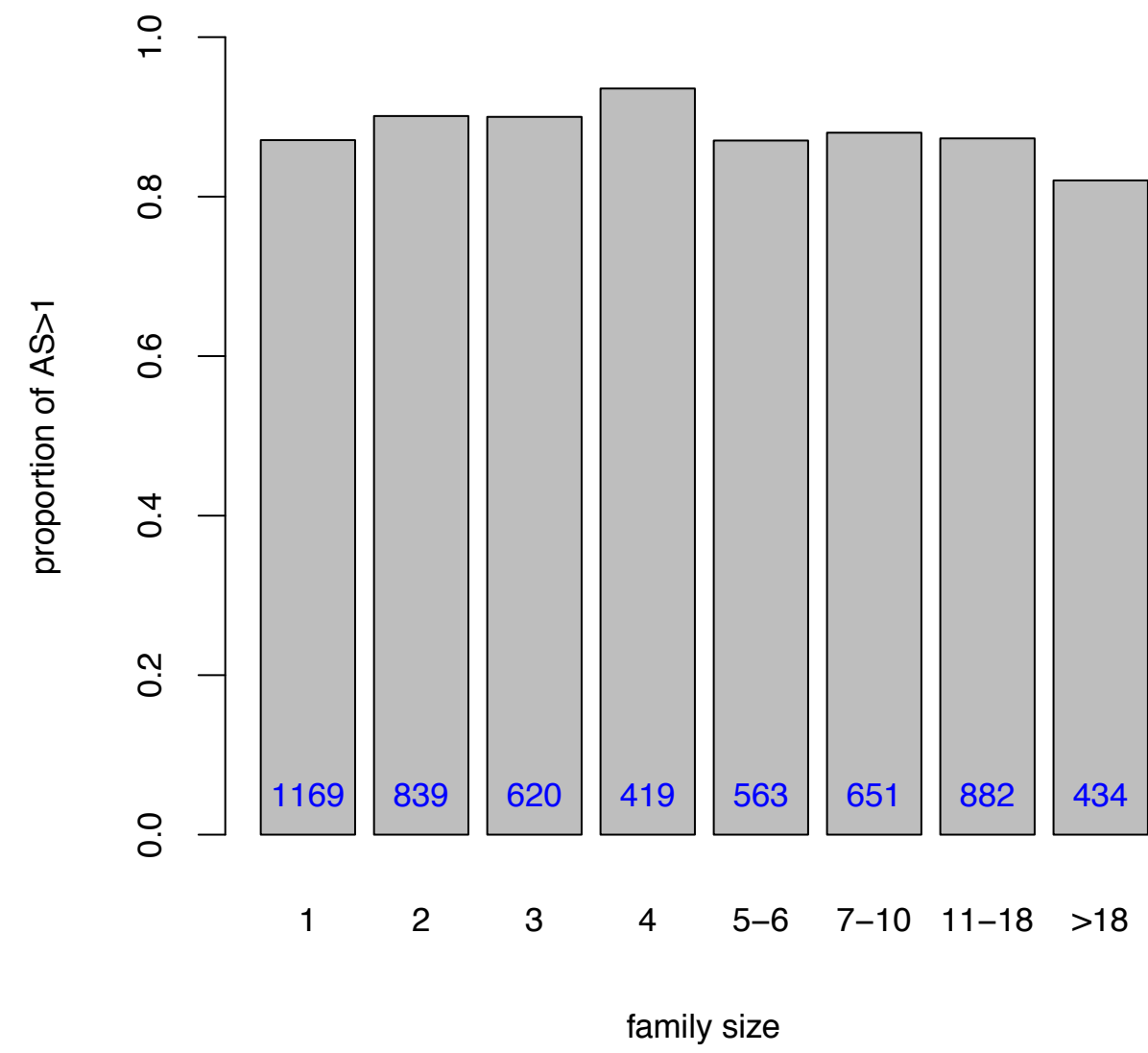


# Figure S11

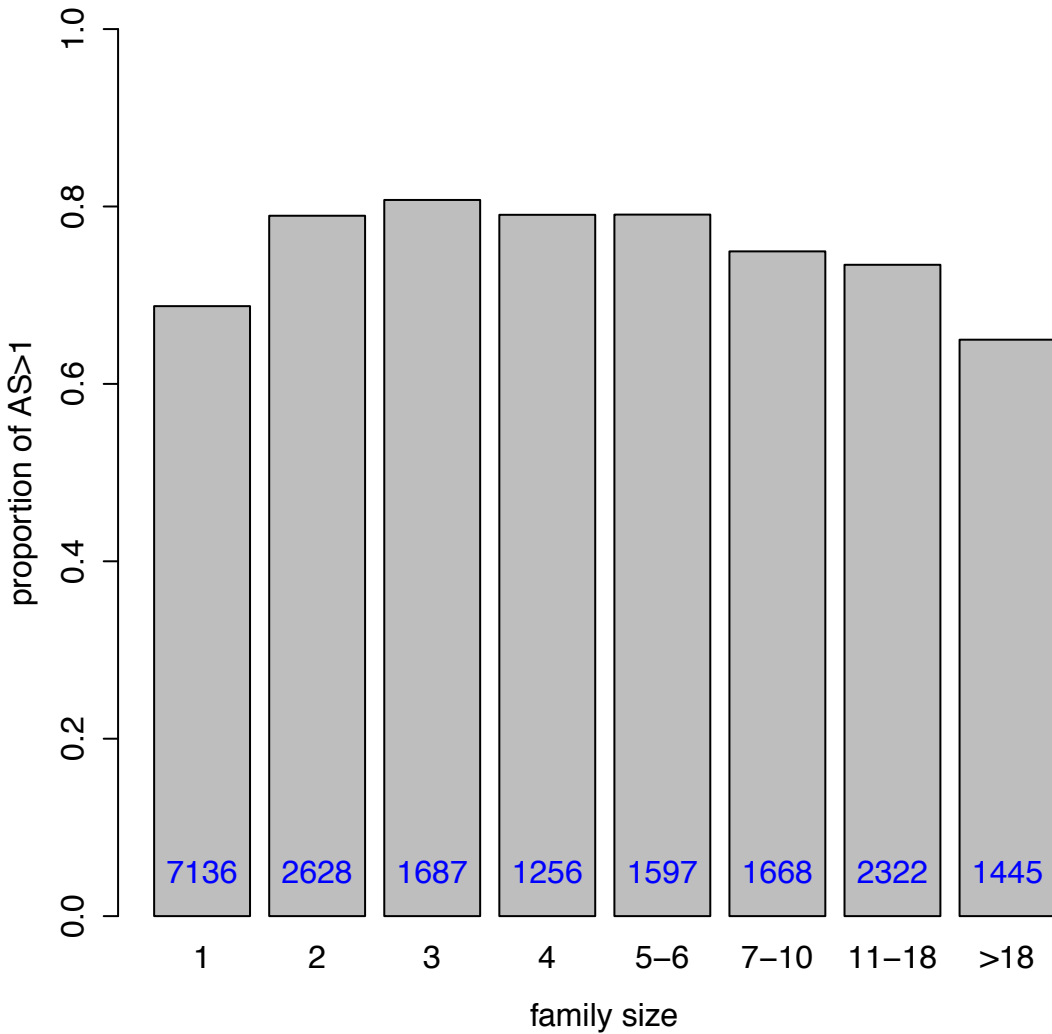


# Figure S12

$r = 0.95 / p = 4.9e-07$

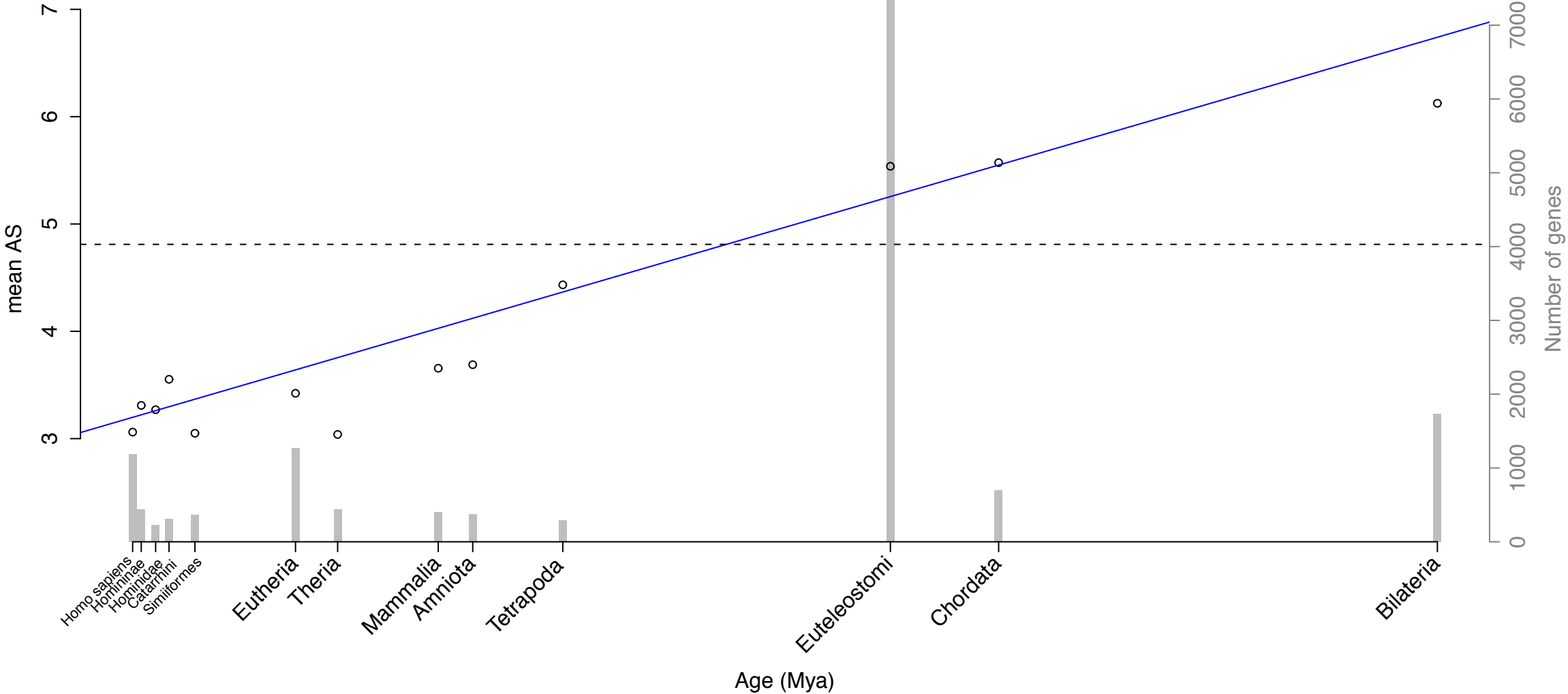
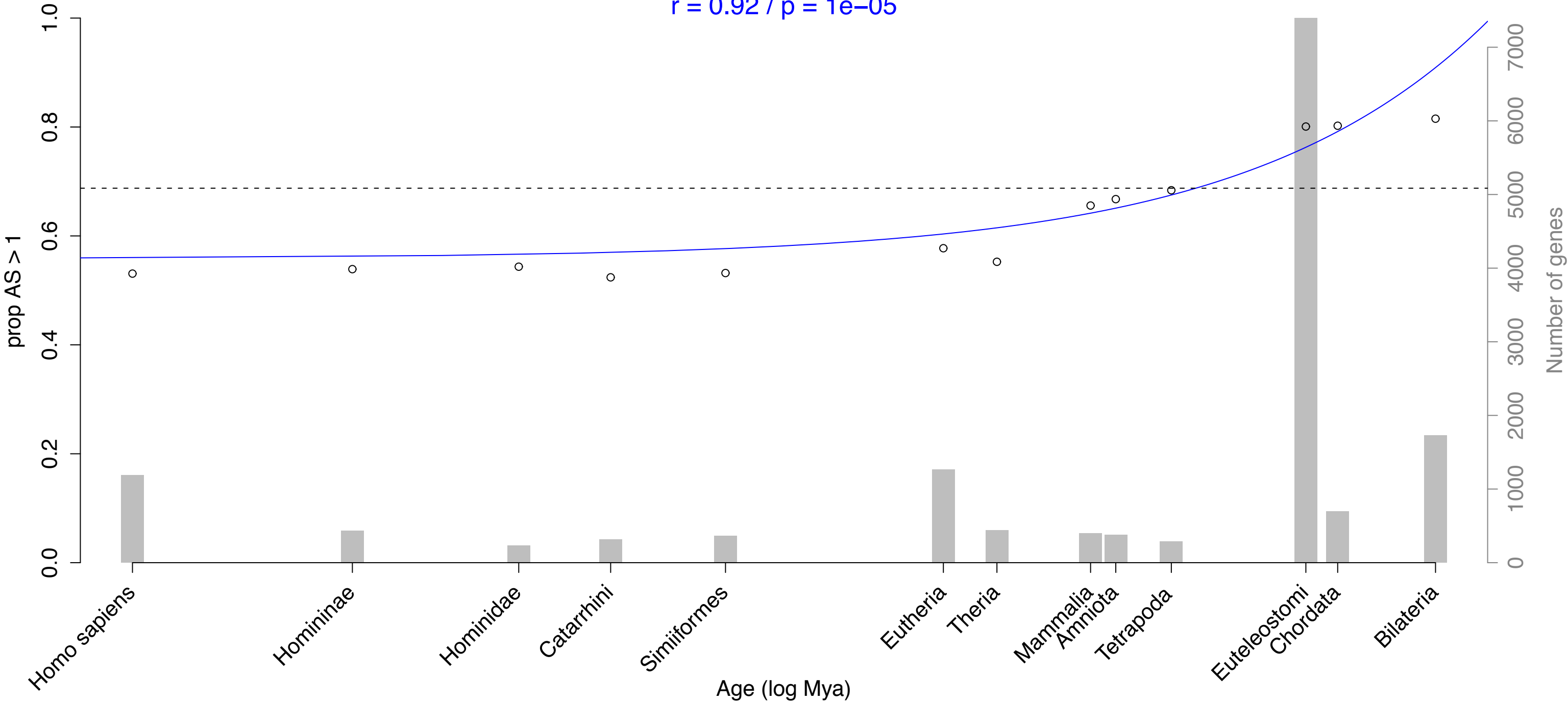
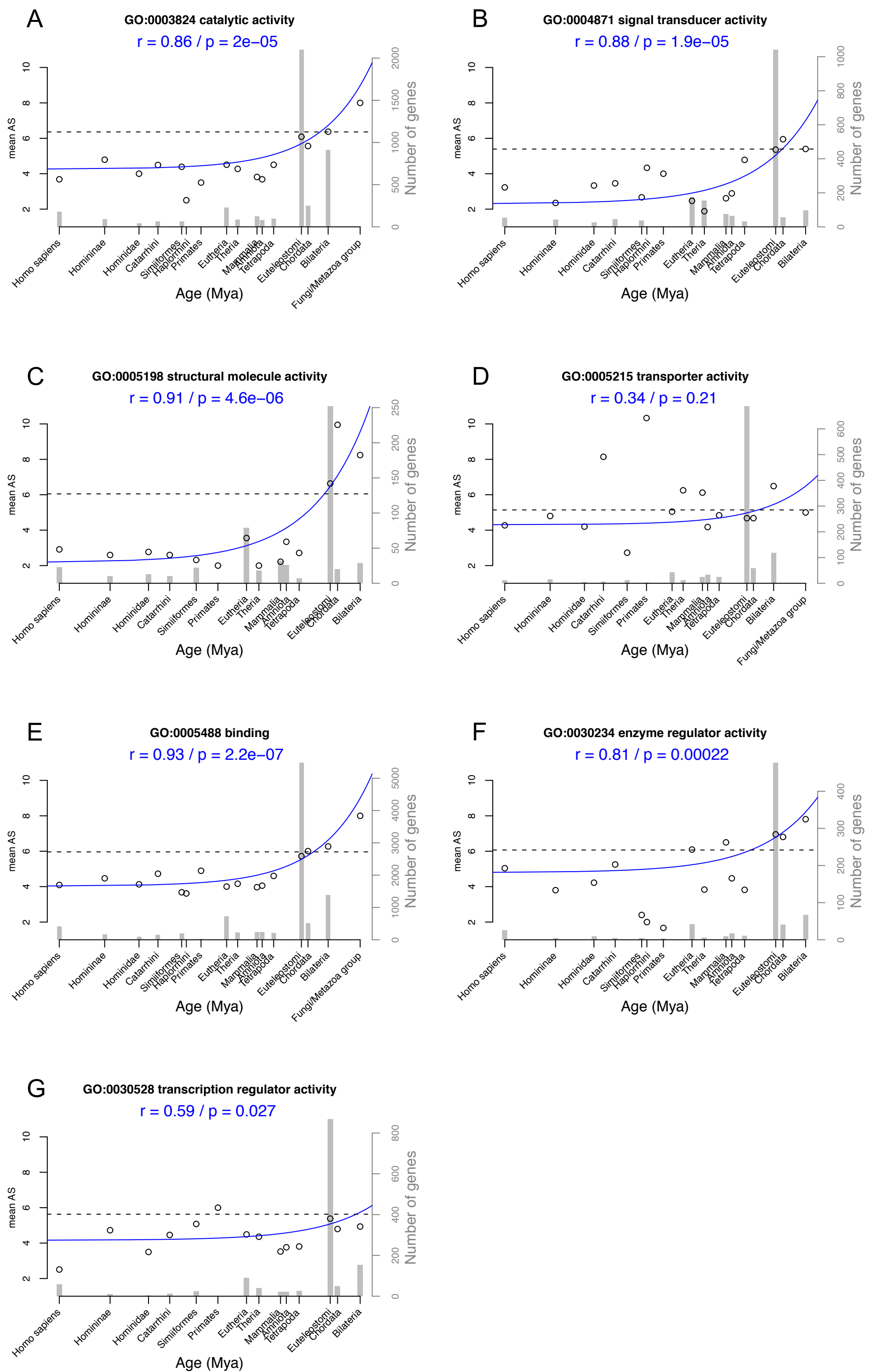


Figure S13

$r = 0.92 / p = 1e-05$



# Figure S14



# Figure S15

$r = 0.97 / p = 5.5e-08$

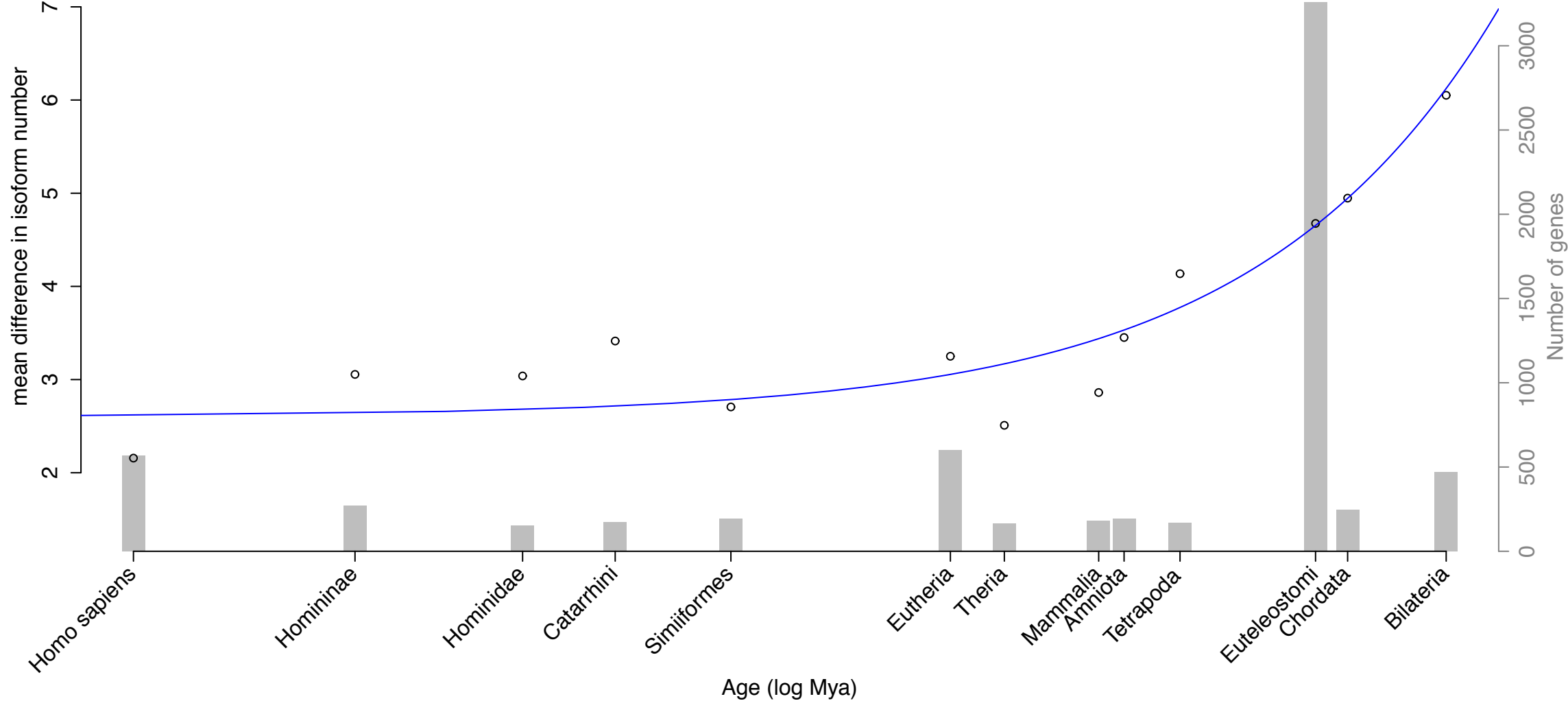


# Figure S16

■ Bilateria  
■ Homo sapiens

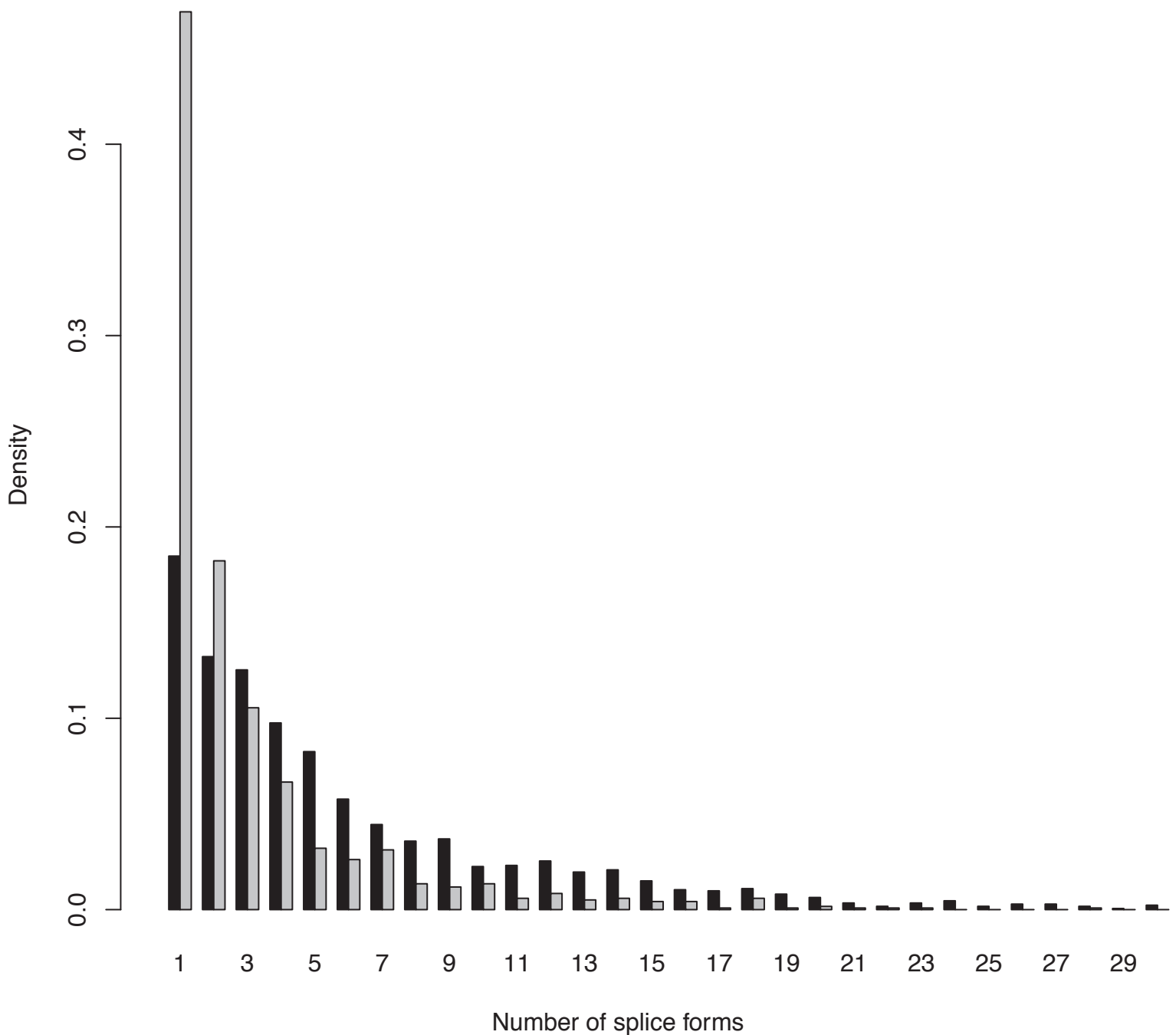


Figure S17

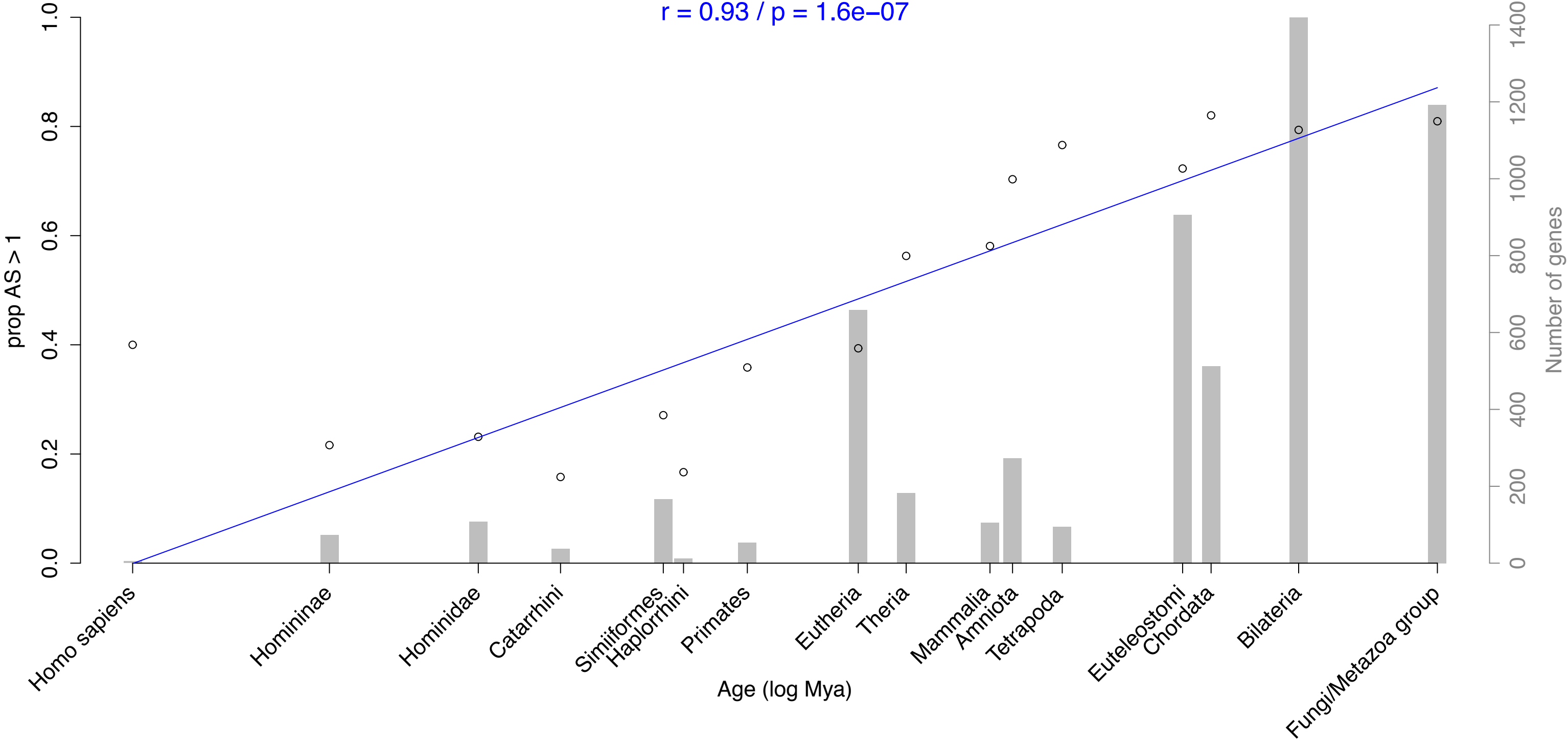
 $r = 0.93 / p = 1.6e-07$ 

Figure S18

$r = 0.95 / p = 1.8e-08$

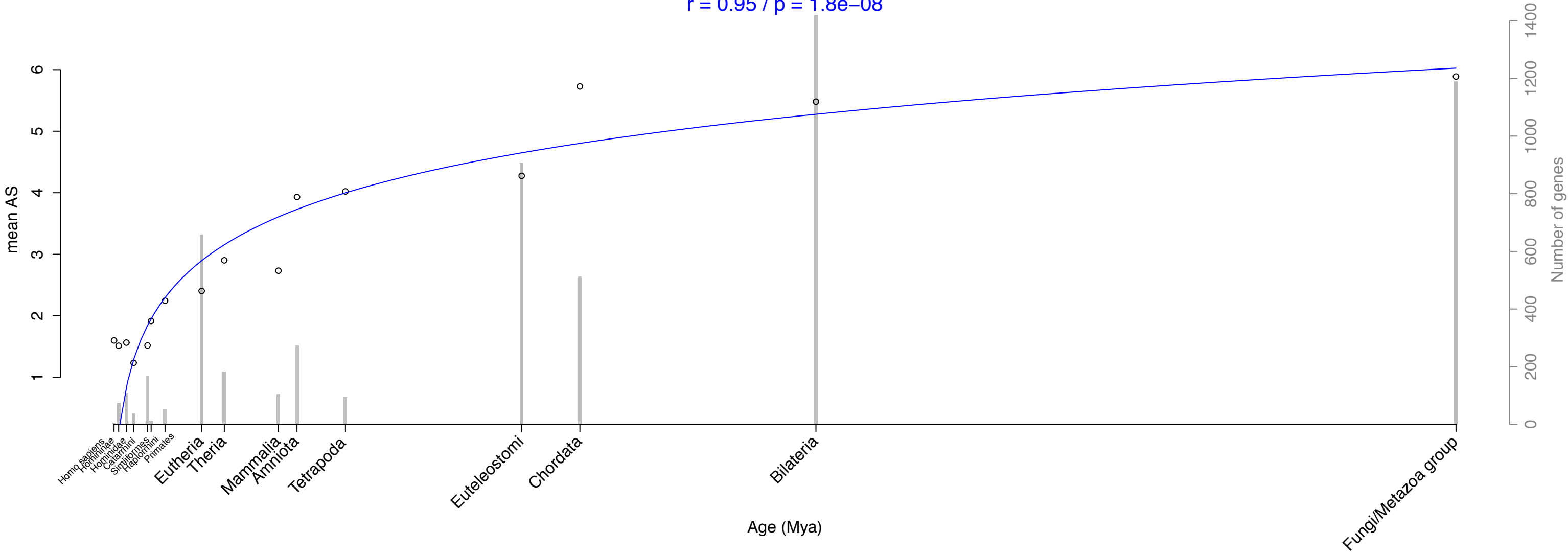


Figure S19

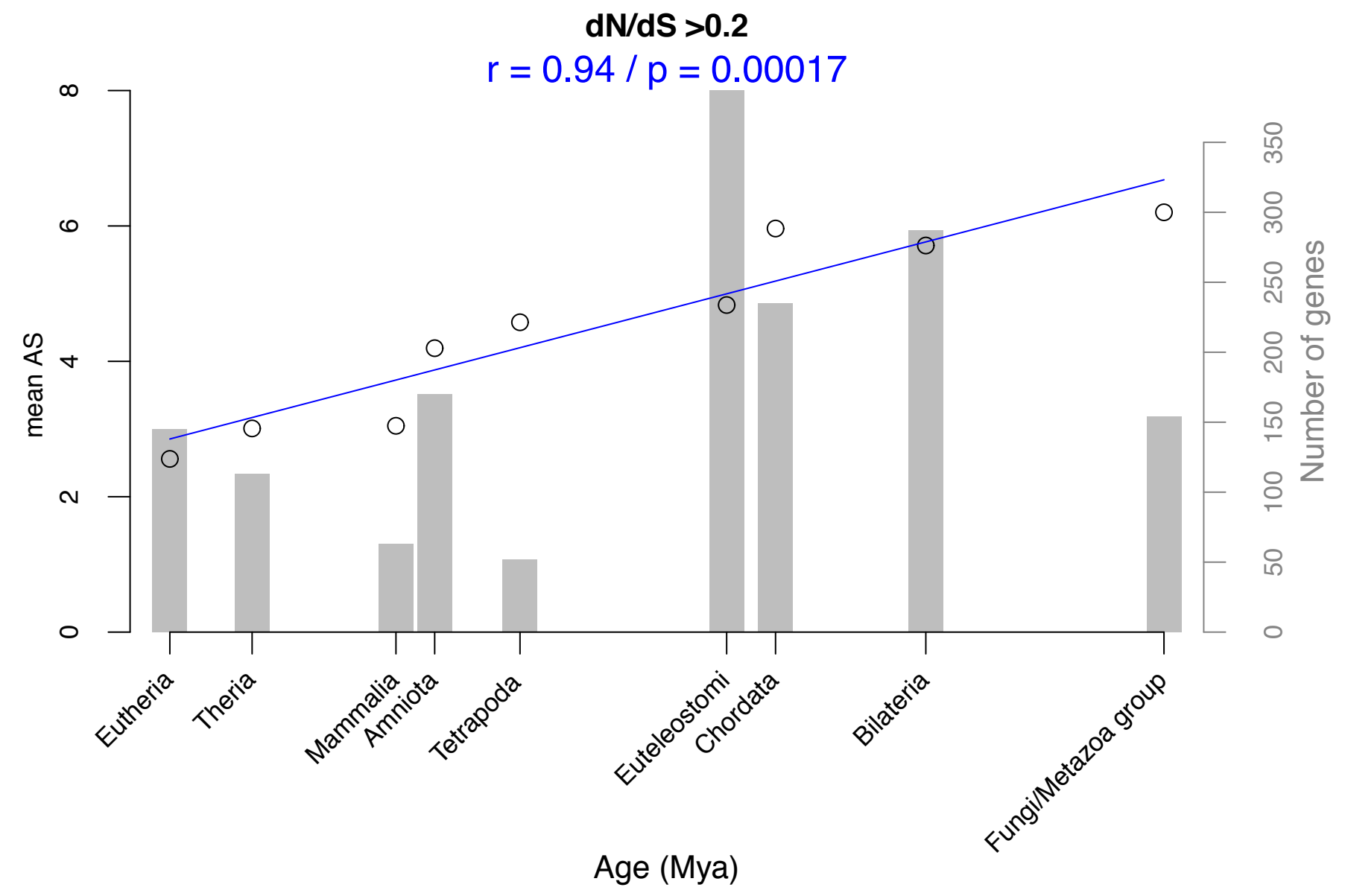
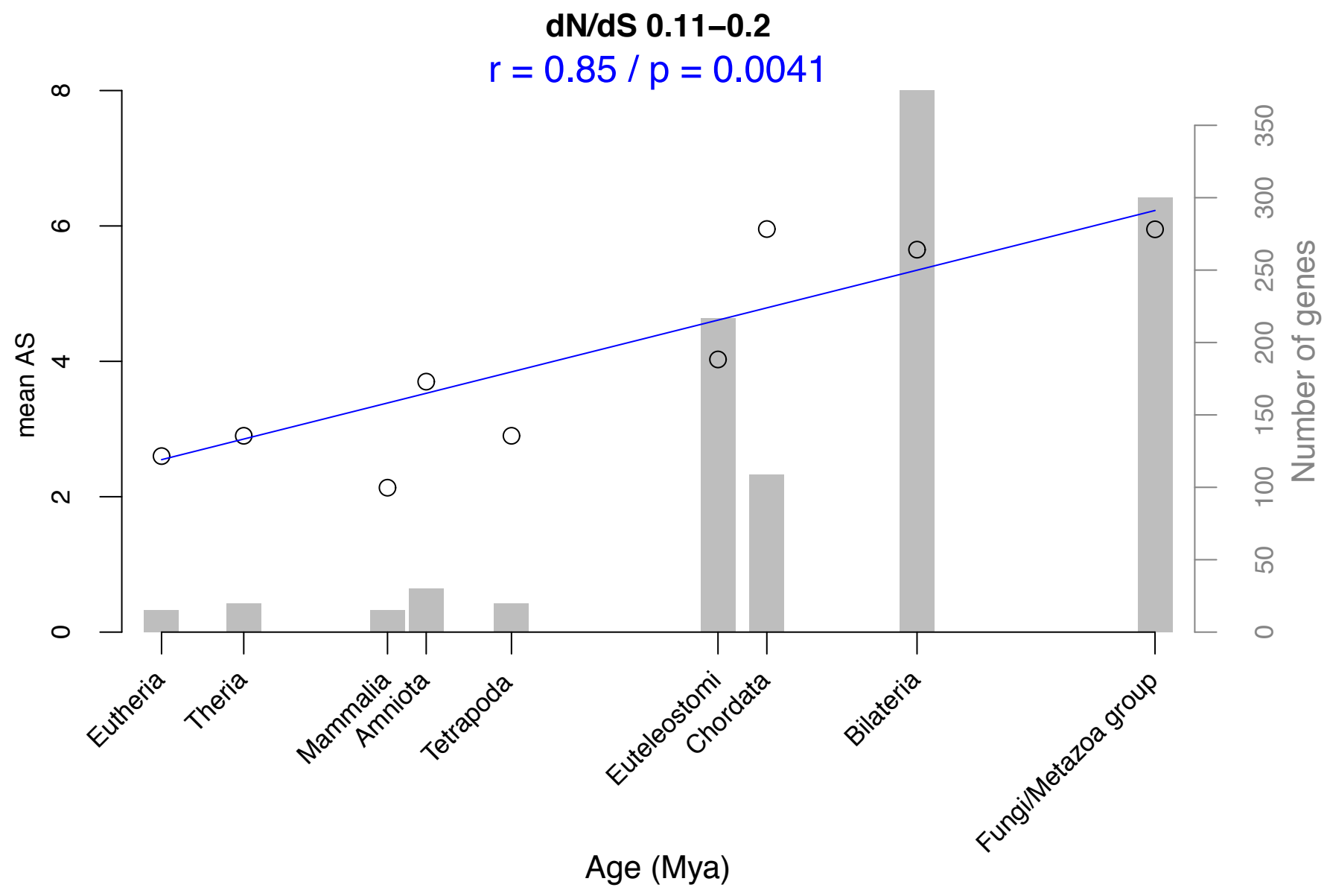
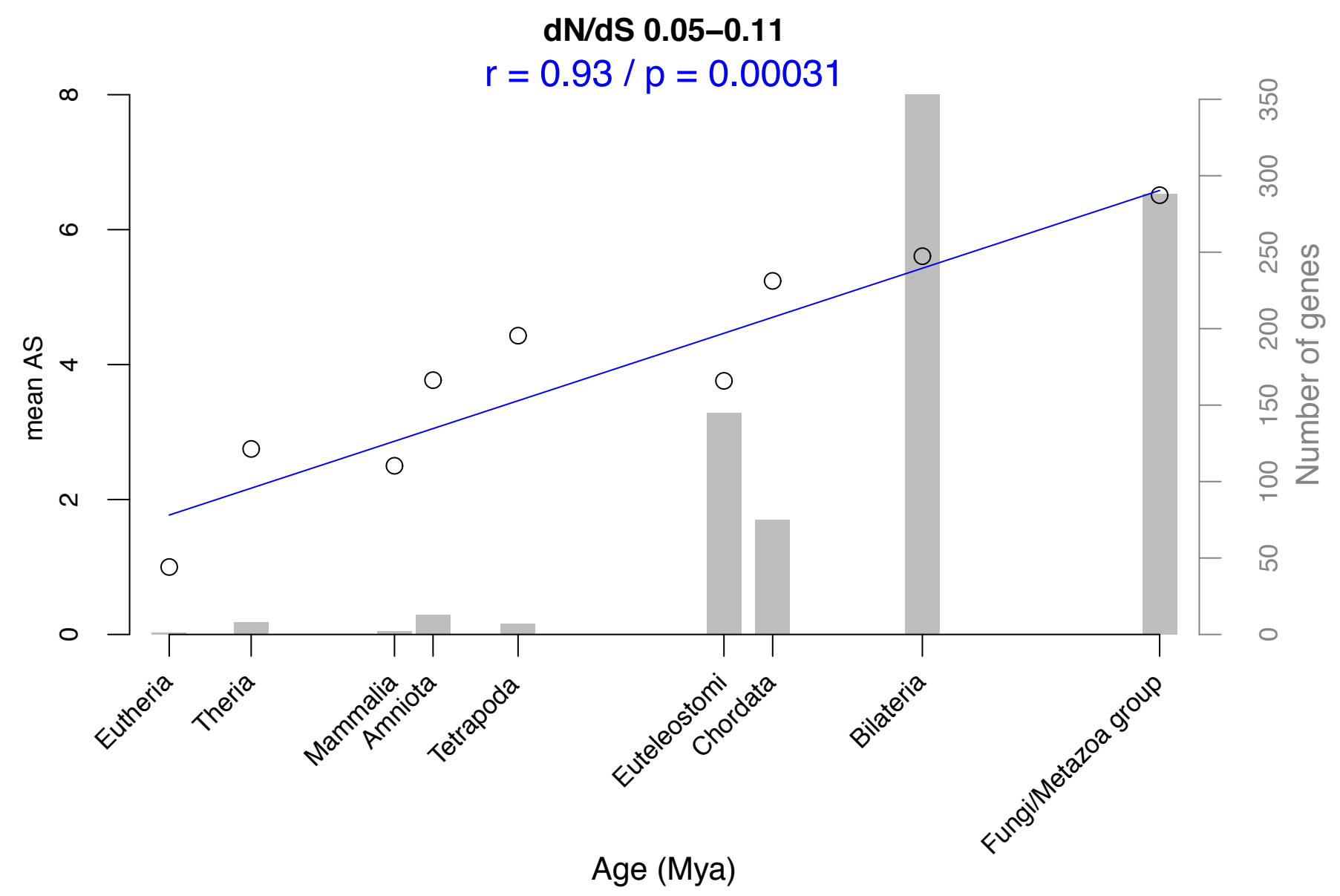
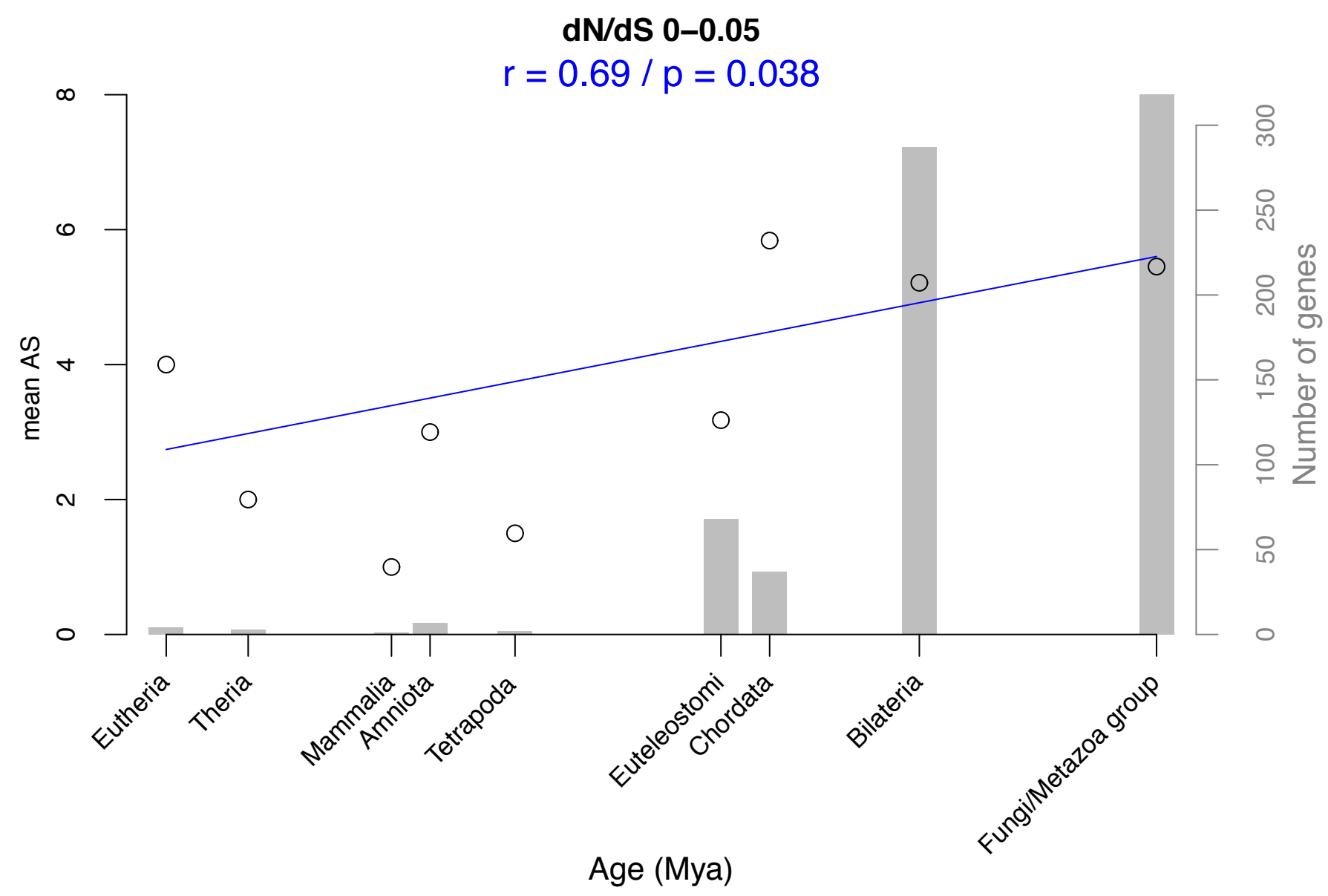


Figure S20

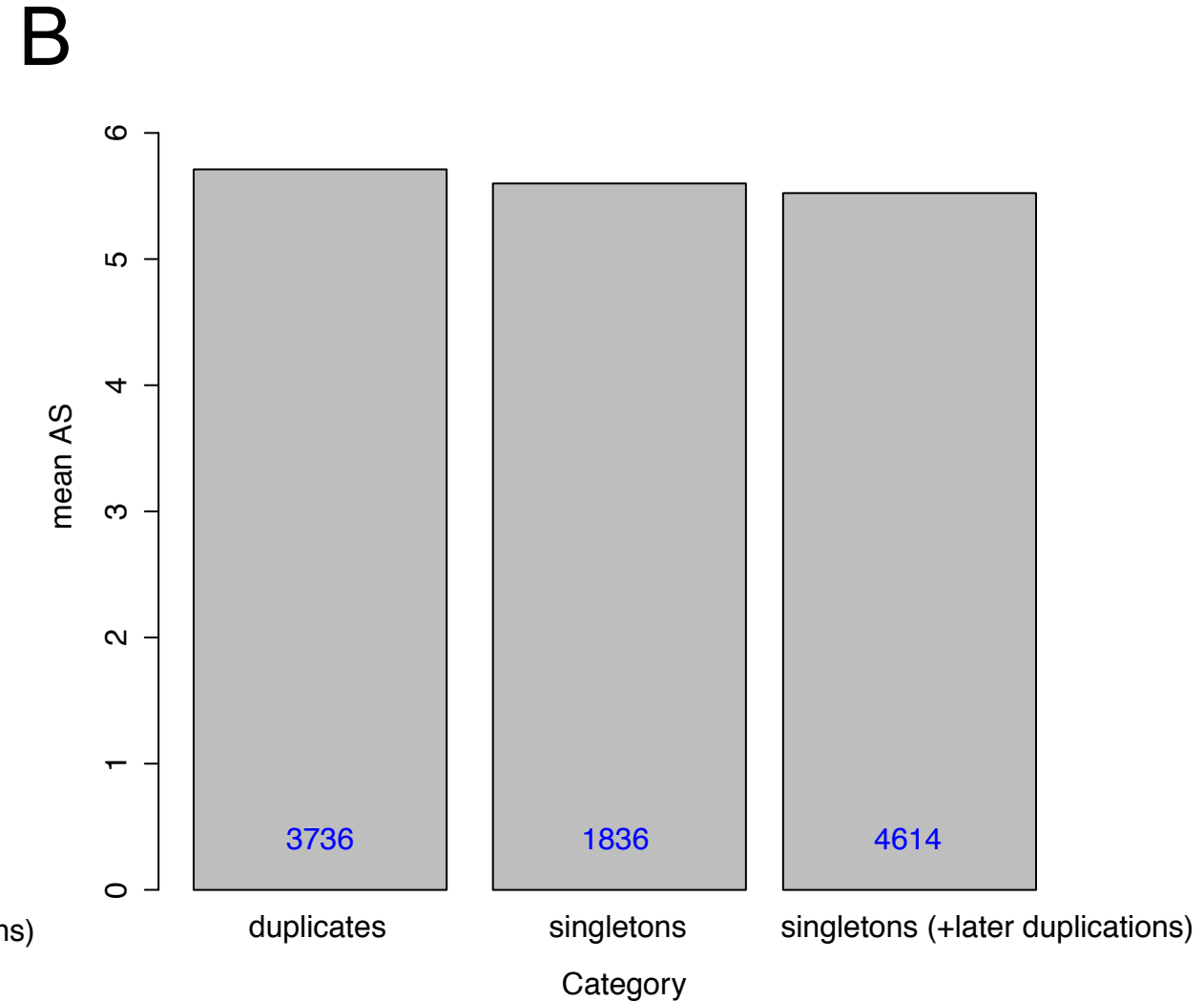
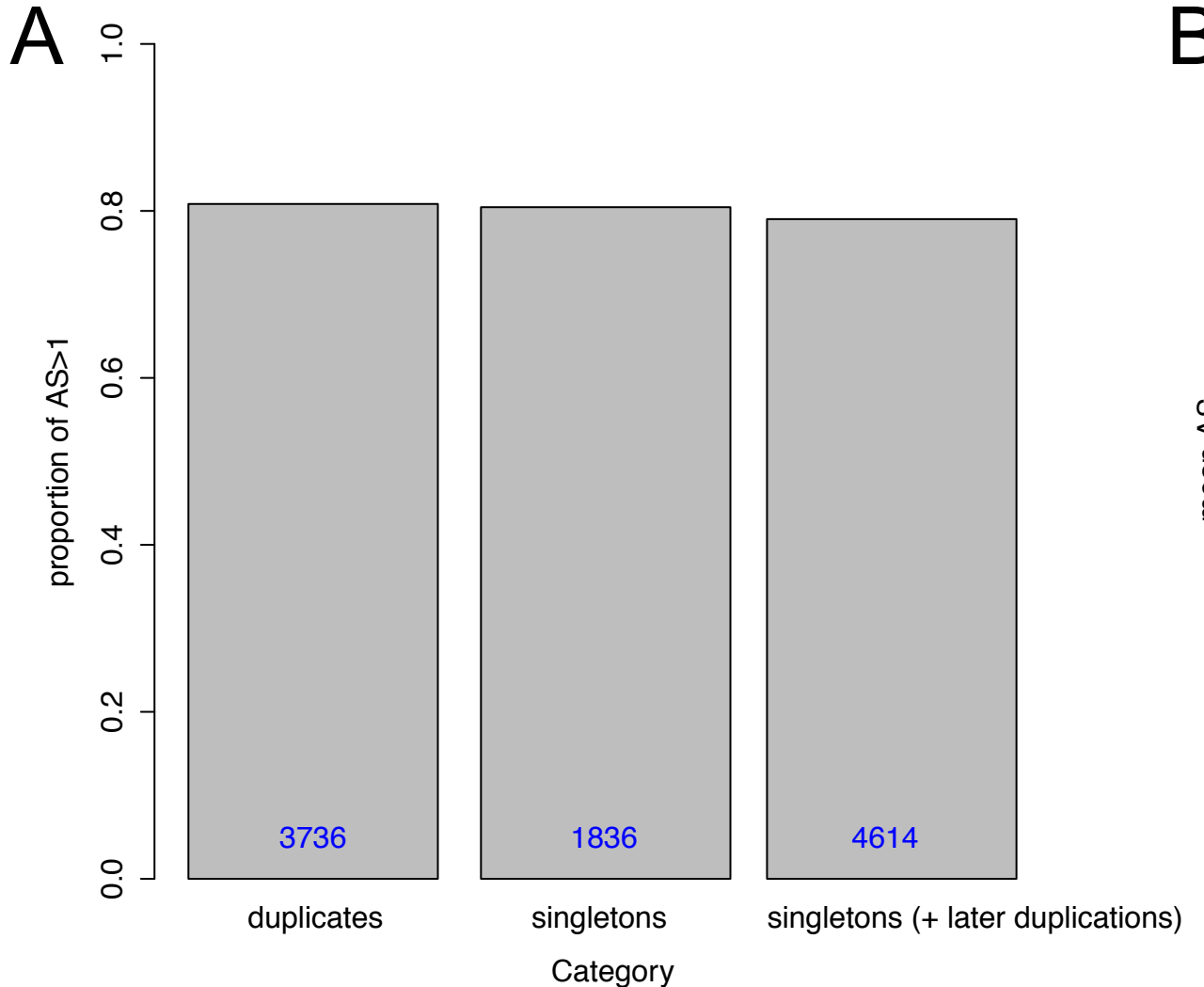


Figure S21

$r = 0.92 / p = 8.3e-06$

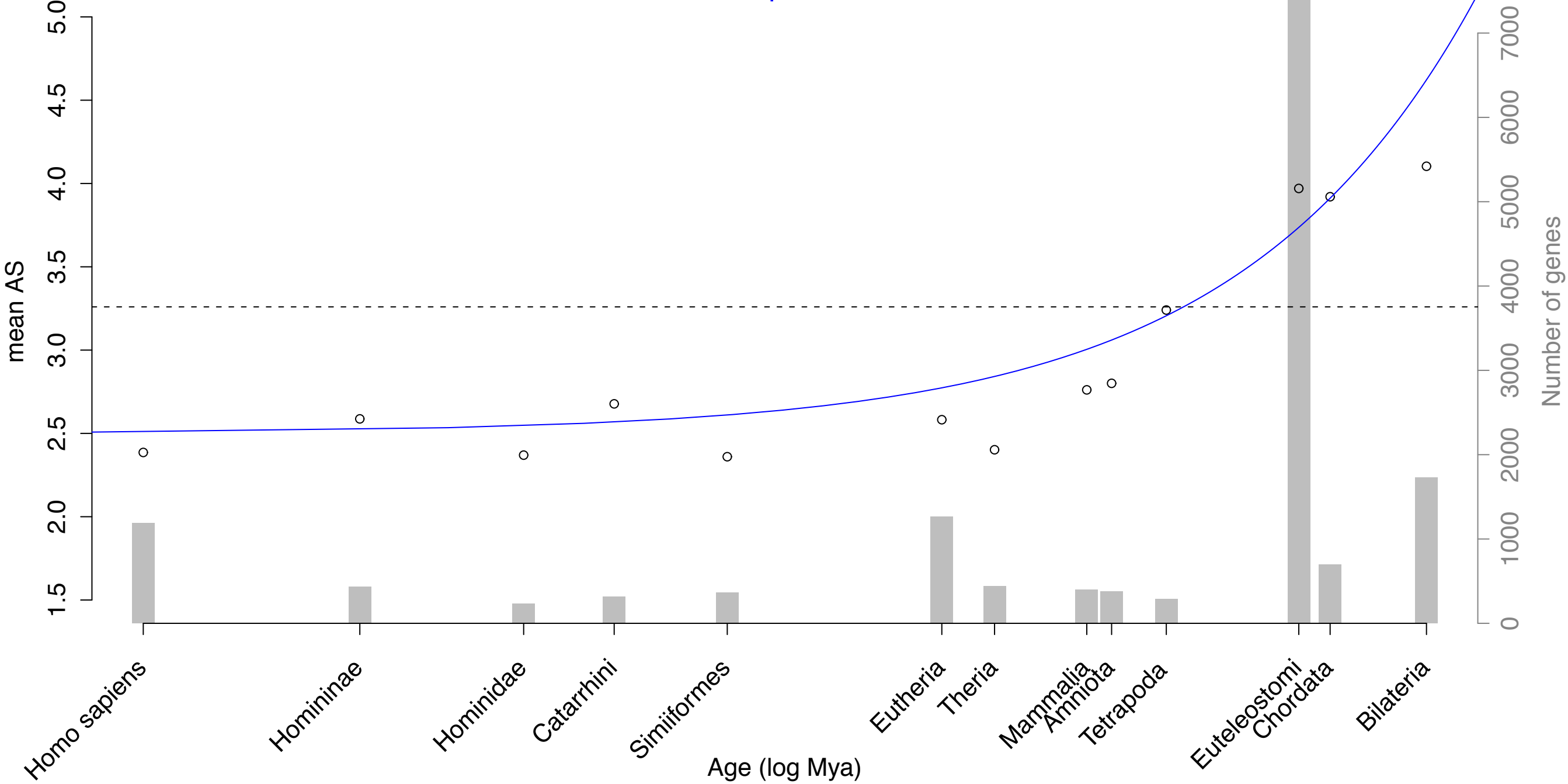
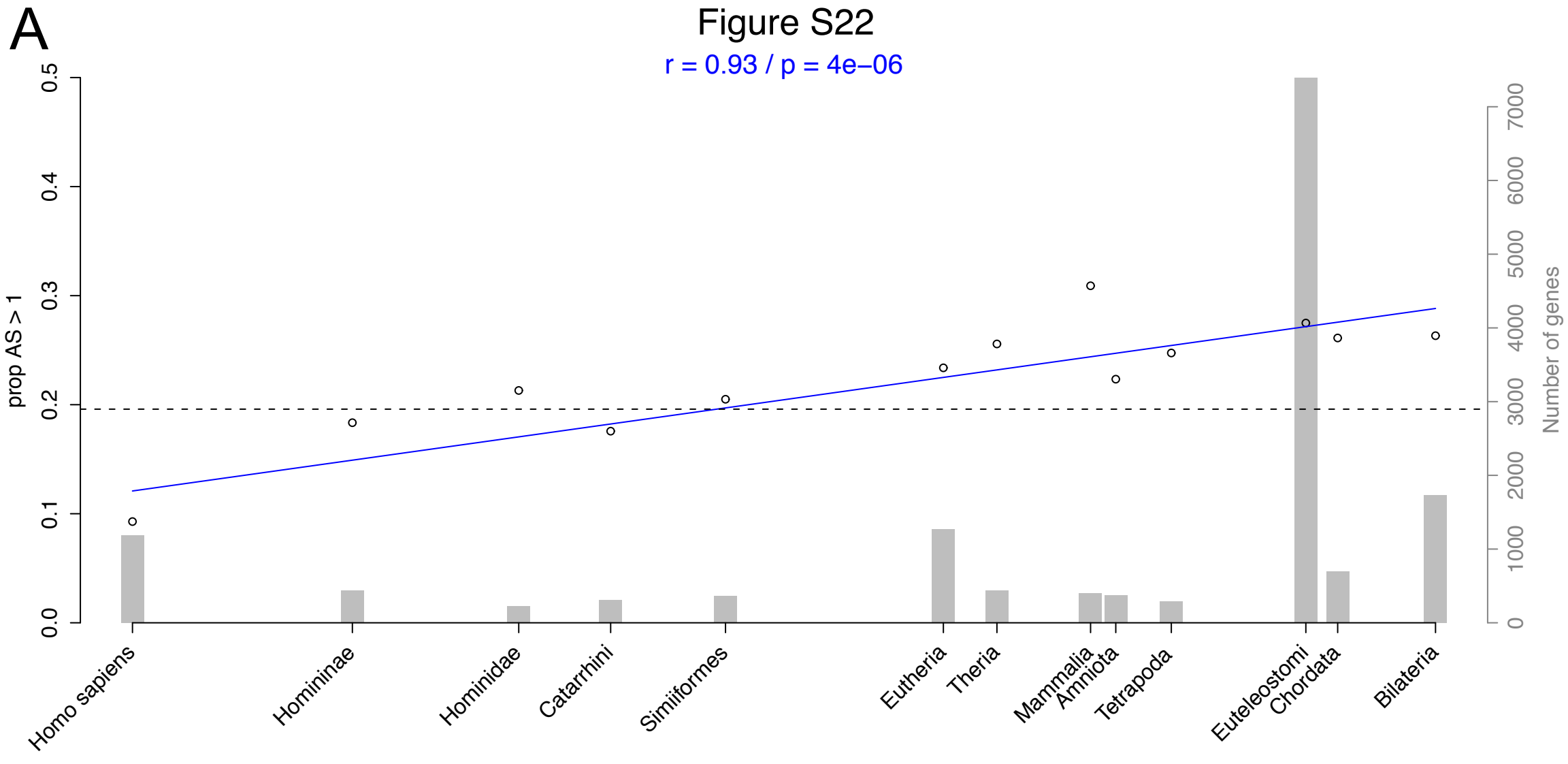
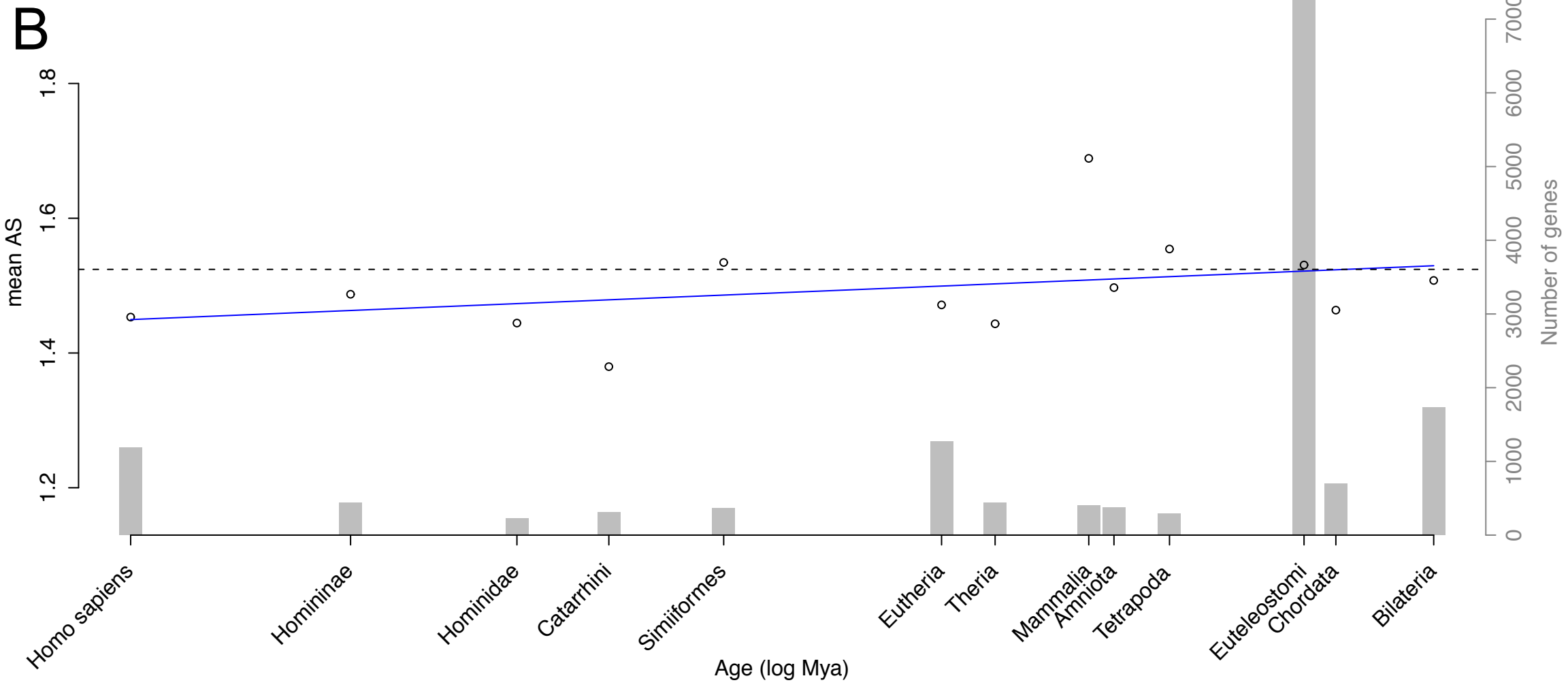


Figure S22

 $r = 0.93 / p = 4e-06$  $r = 0.5 / p = 0.083$ 

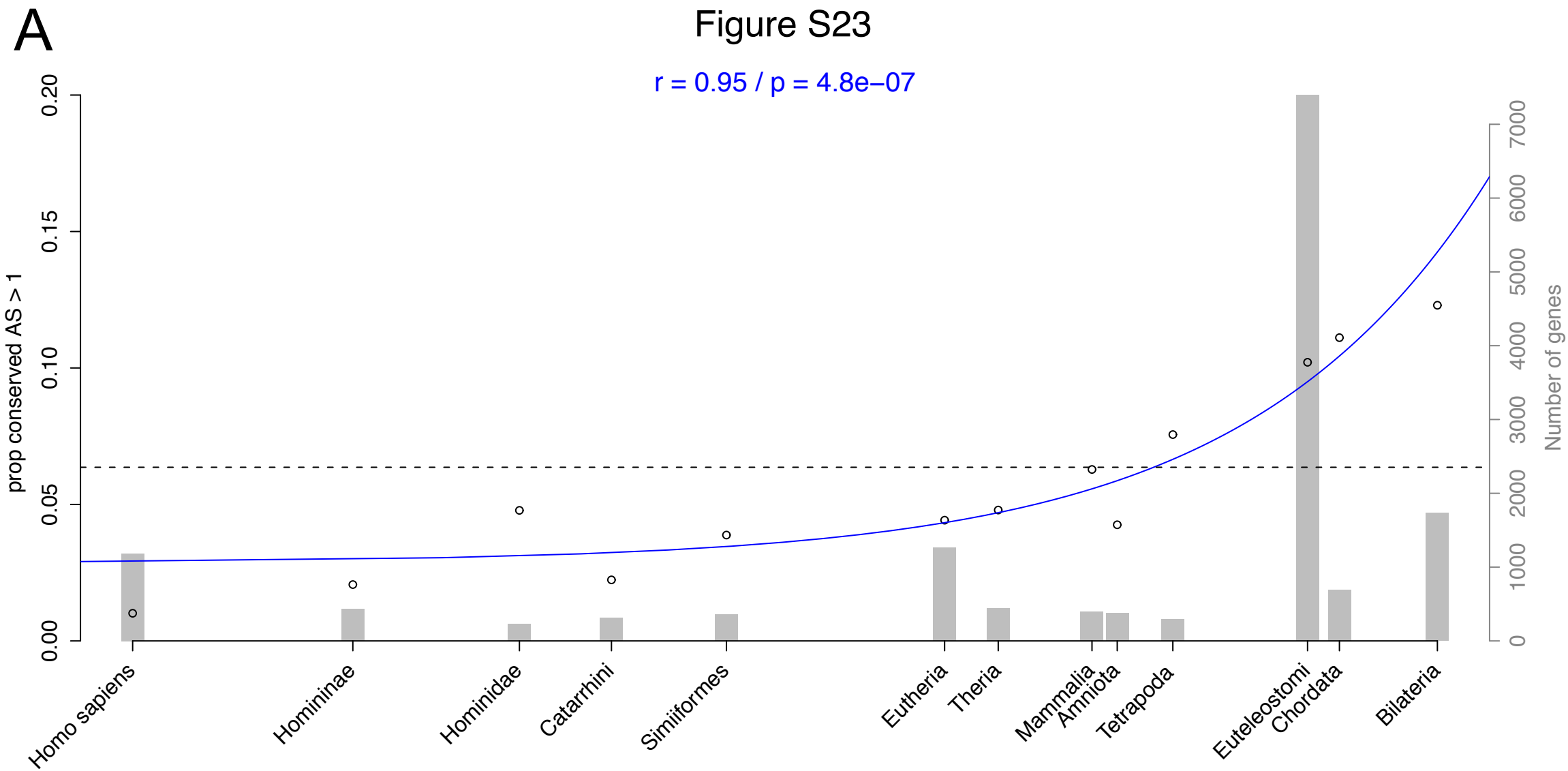
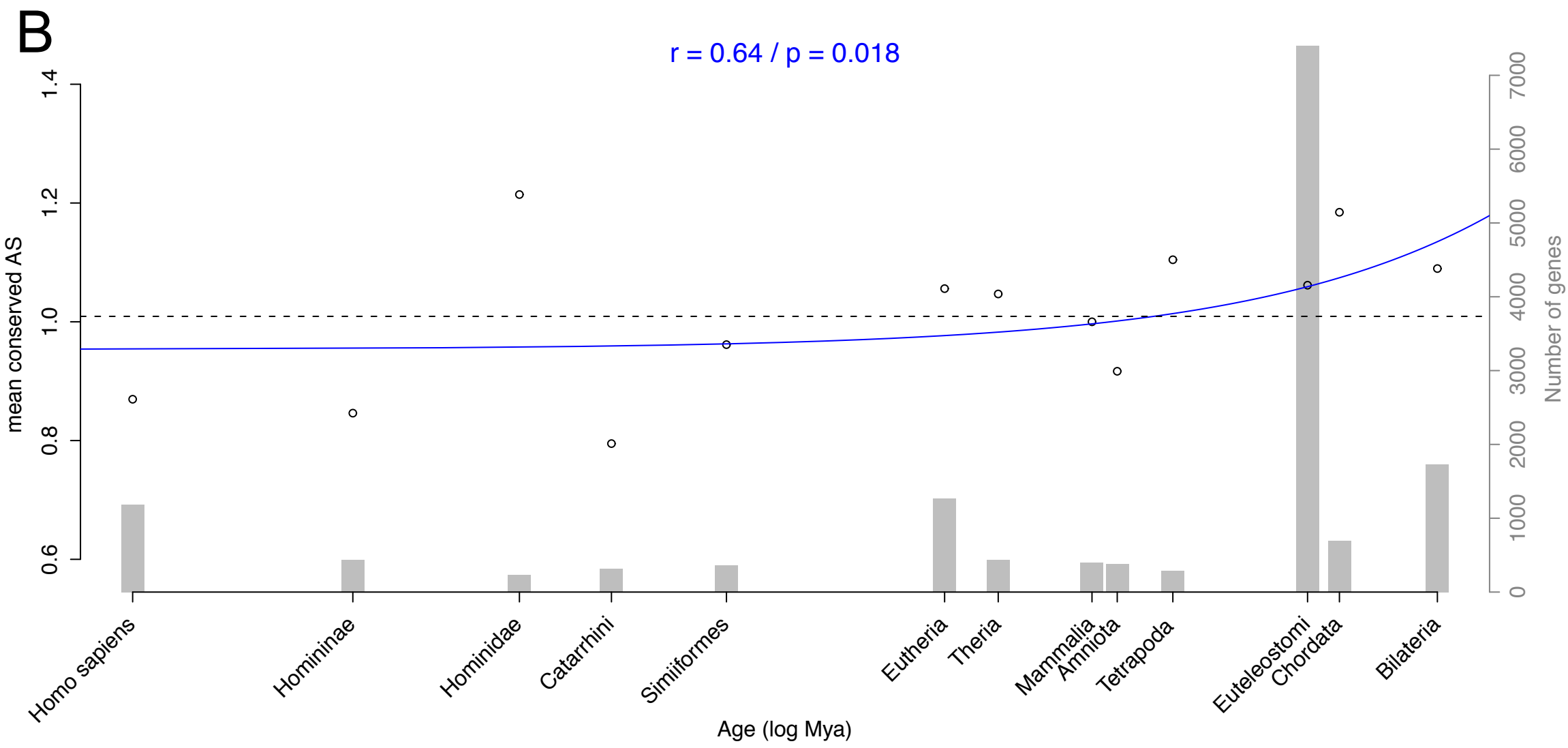
**Figure S23** $r = 0.95 / p = 4.8e-07$  $r = 0.64 / p = 0.018$ 

Figure S24

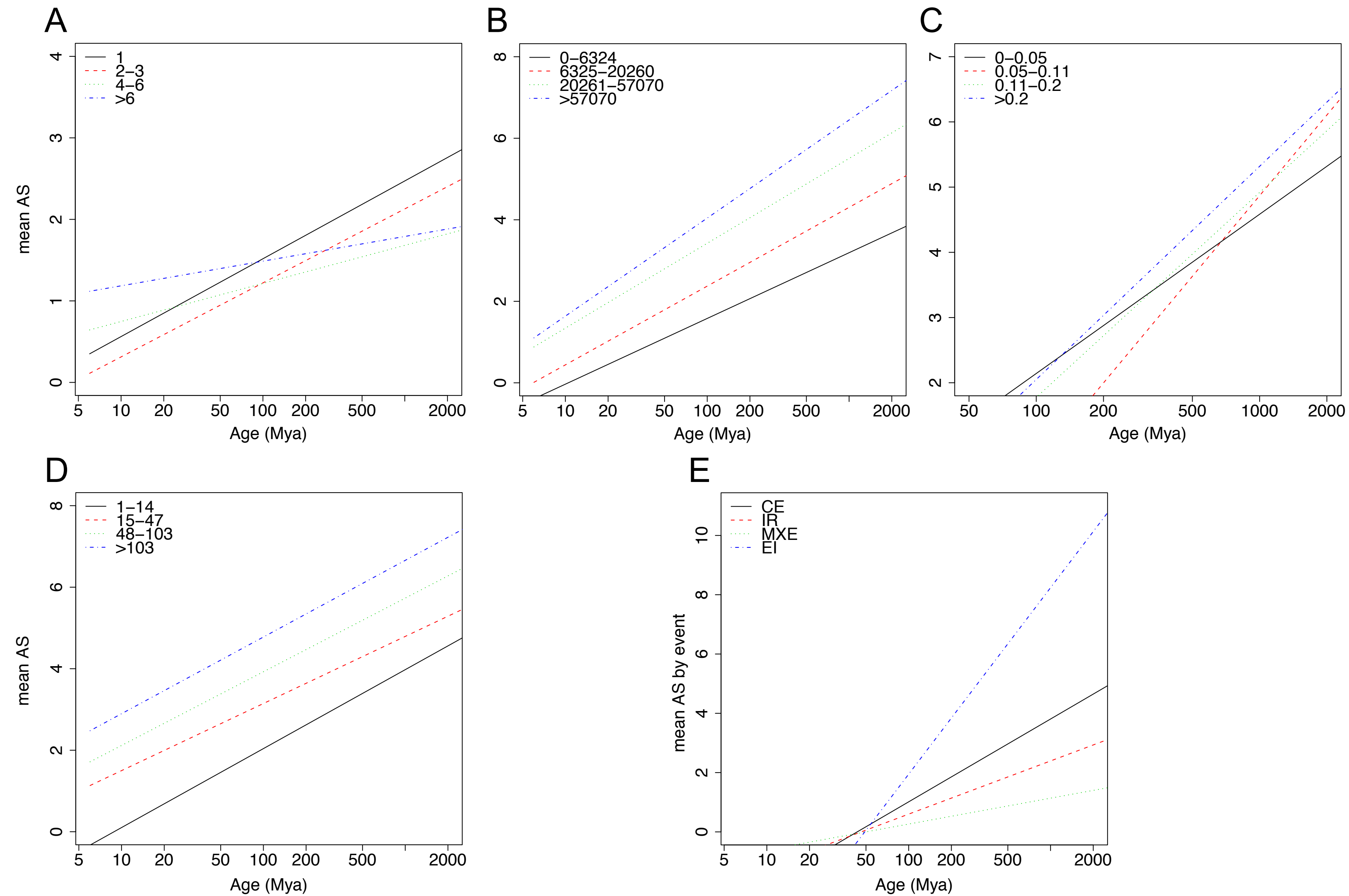
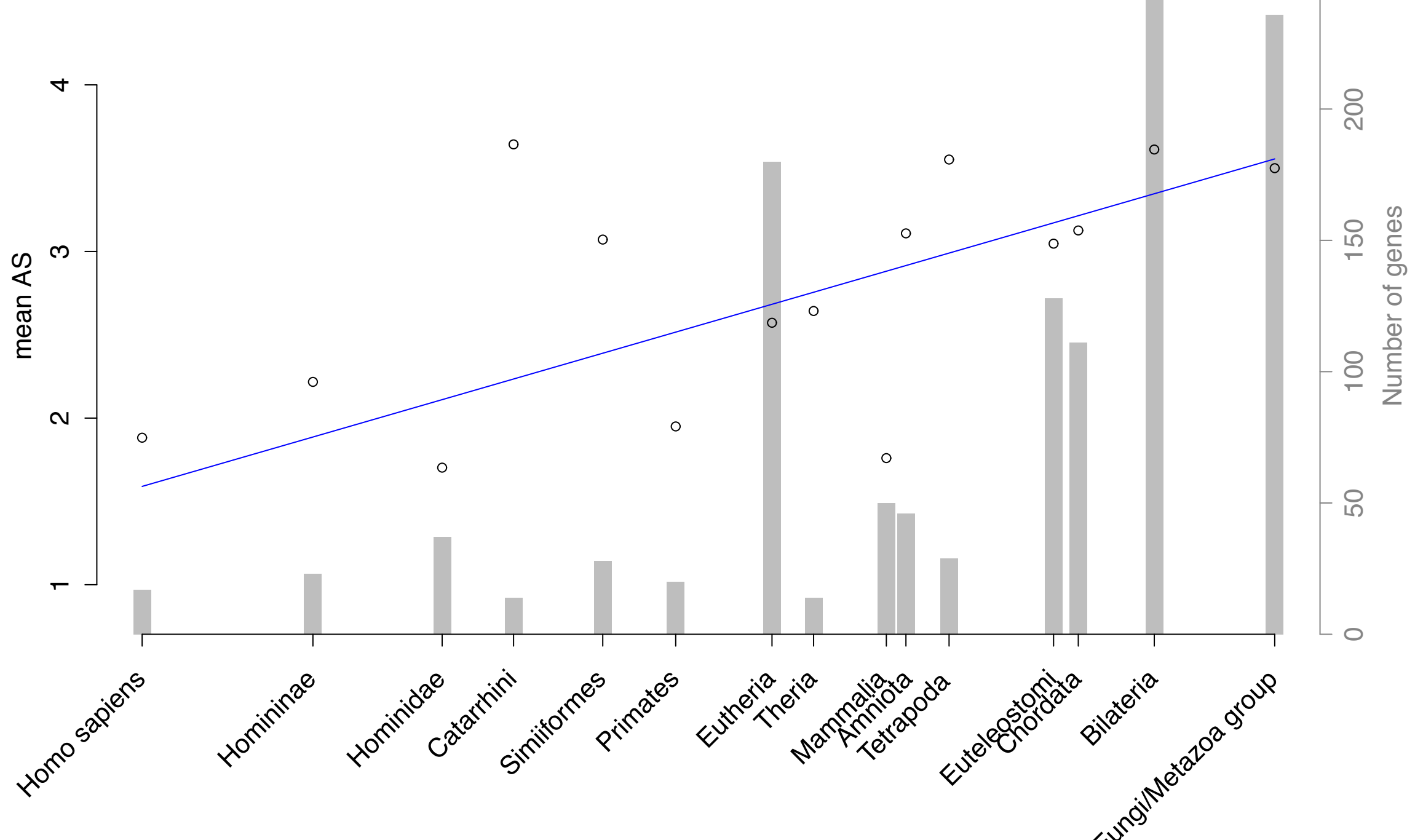


Figure S25

 $r = 0.78 / p = 0.00059$ 

A

 $r = 0.7 / p = 0.035$ 

B

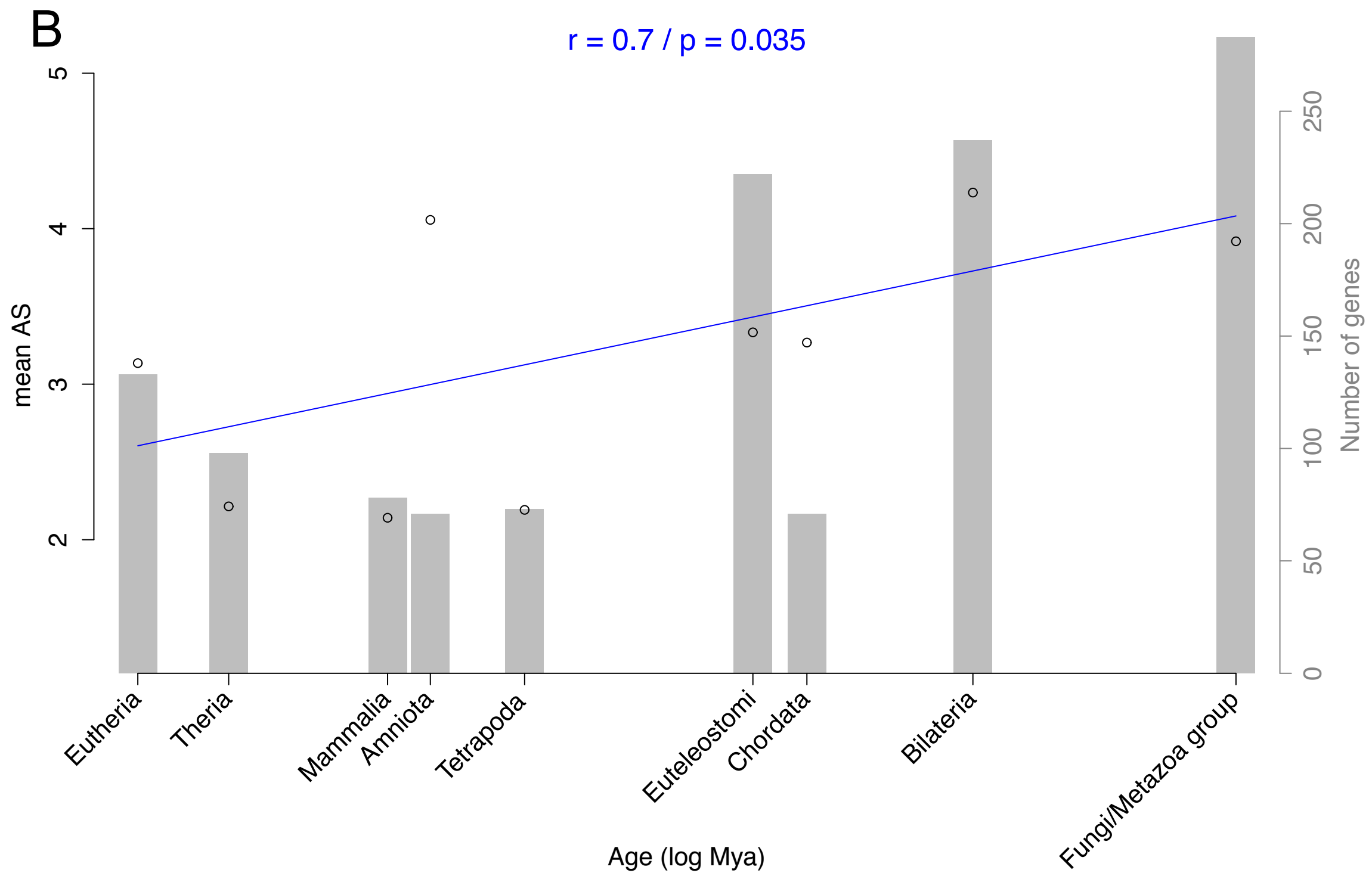


Figure S26

$r = 0.97 / p = 2.1e-05$

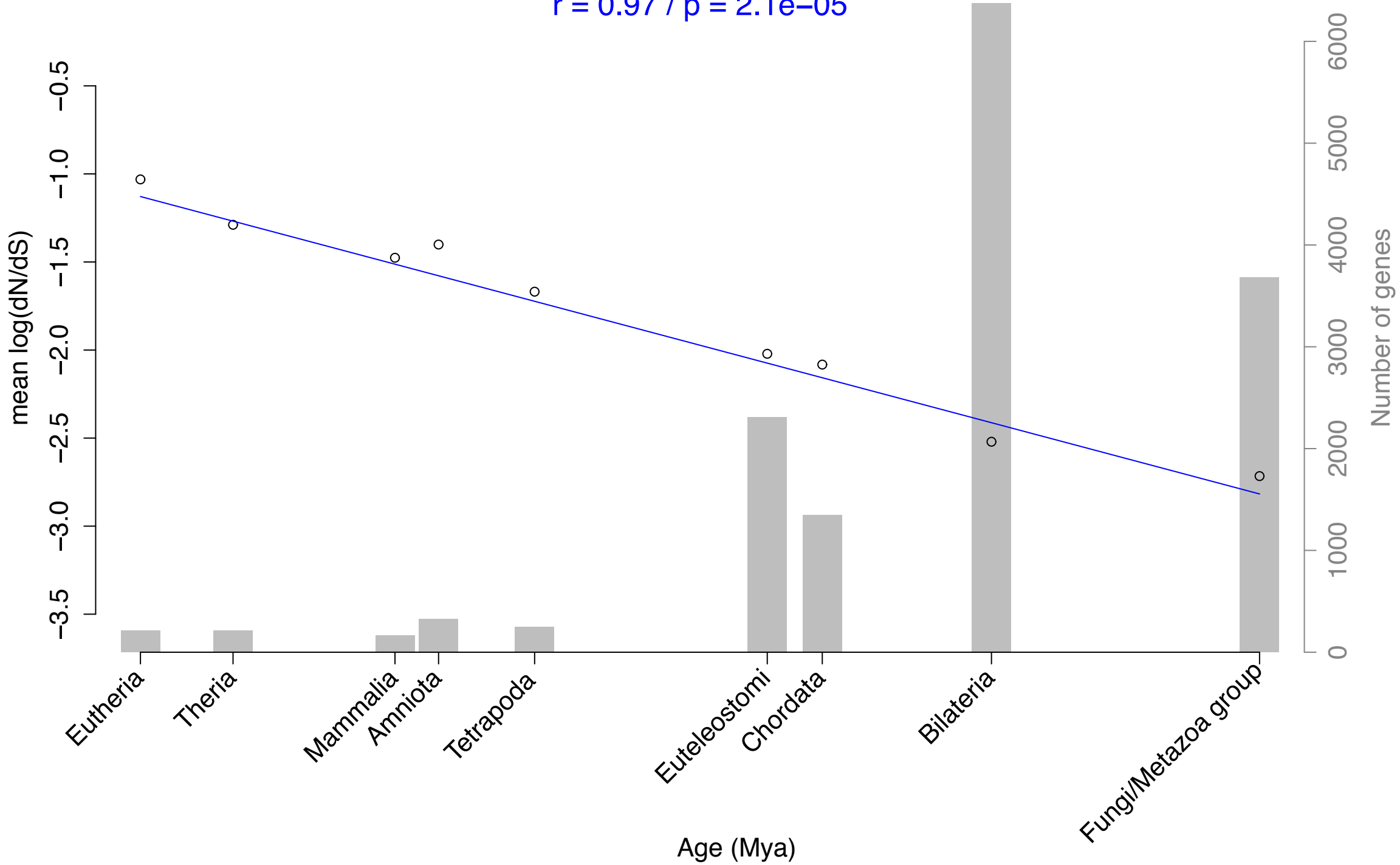


Figure S27

